ADDIS ABABA UNIVERSITY
COLLEGE OF NATURAL AND COMPUTATIONAL SCIENCES
SCHOOL OF EARTH SCIENCES

IDENTIFICATION OF LITHOLOGES AND STRUCTURES IN SERDO, AFAR, ETHIOPIA AND THEIR STATIC GEOLOGICAL MODEL USING REMOTE SENSING AND GIS TECHNIQUES

BY
ADDIS SEID JIBRIL
ID. No: GSR/1356/07

June 2016

A Thesis entitled "**IDENTIFICATION OF LITHOLOGY AND STRUCTURES IN SERDO, AFAR, ETHIOPIA AND THEIR STATIC GEOLOGICAL MODEL USING REMOTE SENSING AND GIS TECHNIQUES**"

Presented to the school of graduate studies of Addis Ababa University
In partial fulfillment of the requirements for the
Degree master of sciences in Earth Sciences
(Remote Sensing and GIS)

By
ADDIS SEID JIBRIL
June 2016

APPROVED BY EXAMINING BOARD: **SIGNATURE**

Dr. K.V. Suryabhagavan _____

Advisor

Dr. Biniam .T _____

Chairman

Dr. Ameha .A _____

Examiner

Dr. Atalay .A _____

Examiner

Acknowledgements

For the purpose of this research work in particular and its masters program study in general, I have interacted, exchanged ideas and also got advice from various people. I have also got cooperation from various organizations. I am very grateful to all of them.

I express my deep sense of gratitude and indebtedness to my Thesis guide Dr. K. V. Suryabhagavan, Associate Professor, School of Earth Sciences, Addis Ababa University, Addis Ababa for his guidance and valuable suggestions during the research work.

I would also like to express my appreciation to Addis Ababa University School of Earth Sciences, Graduate Studies staff members and libraries for their providing of the necessary references, equipments and assistance for my study.

I am greatly indebted to all my family members for their helpful nature throughout my assignment and material support throughout my life. But for their cooperation, I would not have completed this thesis in time.

My whole hearted thanks are also due to all my friends, whose names could not be mentioned separately because of limitations; for their constant encouragement and cooperation. I am thankful to the almighty for the divine blessings showered up on me to complete this work.

DEDICATED TO: MY FAMILY WITH LOVE!

Table of Contents

List of Tables

List of Figures

List of Abbreviations

ASTER Advanced Space borne Thermal Emission and Reflection Radiometer

DEM Digital Elevation Model

DIP Digital Image Processing

DN Digital Number

EARS East African Rift System

EMR Electromagnetic Radiation

EO Earth Observatory

ETM Enhanced Thematic Mapper

FCC False Color Composite

GIS Geographic Information System

IARR Internal Average Relative Reflectance

ICA Independent Component Analyses

HIS Intensity Hue Saturation

MER Main Ethiopian Rift

MSS Multispectral Scanner

NIR Near Infrared

OIF Optimum Index Factor

OLI Operational Land Imagery

PCA	Principal Component analyses
RS	Remote Sensing
SNR	Signal to Noise Ratio
SRTM	Shuttle Radar Topographic Mission
TIRS	Thermal Infrared Sensor
USGS	United States Geological Survey
VSWIR	Visible Short Wave Infrared Ray

Abstract

New generations of advanced remote sensing data have been used by Earth scientists over last decades. This study presents the applicability of recently launched Landsat 8 and Shuttle Radar Topographic Mission digital elevation model data for lithology and structure mapping. Processing of multispectral medium resolution of landsat 8 and digital elevation model data were used for detection and mapping lithology and structure in the Serdo area. These data have been processed and interpreted with the production of lithologic and structural map, at a scale of 1:100,000. The results revealed that lithologic features and their textural characteristics are easily identified by coastal/aerosol, visible, near-infrared and short wave infrared (1-7) bands with resolution merge of band 8 (pan) bands. Spatial enhancement of landsat 8 data using convolution filters (spatial domain of the image) and digital elevation model (DEM) extracted from the SRTM have been used for structures extraction. Hill-shading techniques are applied to SRTM DEM's to enhance terrain perspective views and to extract morphologically defined structures. Faults and different set of fracture systems are major structural elements recognized. Six main lithologic types and 1859 structures are identified and totally12321 km^2 area was mapped in this work.

Keywords: Landsat 8, lithology, DEM, NIR, Structures, Spatial Enhancement.

CHAPTER I

BACKGROUND OF THE STUDY

1 Introduction

Mapping lithology and structures require cumbersome fieldwork investigations. However, fieldwork is usually time consuming and may take up years to complete, depending primarily on the extension and/or the accessibility of the area under investigation. Multispectral satellite remote sensing technology provides a relatively efficient and low cost method for the geological mapping of terrains that are geologically complex or poorly or expensively accessible. Remote sensing data, such as aerial photographs and multispectral imagery data can provide more continuous and detailed information and quantitative interpretations can be made for large areas, thus enabling even the most inaccessible terrain to be mapped. However, the results of a digital image processing and analysis require a field investigation in some selected testing areas in order to estimate the accuracy of the geological interpretation. According to Drury, (1987) remote sensing has the advantage of providing synoptic overviews of the region thus it may directly pinpoint the characteristics of structures and geological features extending over large areas. As opposed to fieldwork investigations, remote sensing along with image processing techniques accounts for a less time consuming and a more cost effective method for lithology and structure investigation. Nonetheless, such techniques in no way replace field investigations, but on the contrary they complement each other. According to Laake, (2011) using Landsat multi-band RGB (7,4,2) distinguished clearly between the basement rocks, the Mesozoic clastic sedimentary rocks and coastal carbonates, while the difference between bands 4 and 2 highlighted difference in lithology between pure limestone and more sand cover. The use transformed data space using methods such as PCA and ICA, help to decor relate band information while separating data along new component lines which can further be enhanced by visualizing the new components in FCC. Other analyses which have been utilized are neural networks (Harris et al., 2001) and use of DEM to aid lineament extraction (Chaabouni *et al*., 2012; Favretto *et al*., 2013). Lineament mapping is an important part of structural geology and they

reveal the architecture of the underlying rock basement (Ramli *et al*., 2010). Lineament (structures) extraction involve both manual visualization and automatic lineament extraction through softwares such us PCI GeoAnalyst, Geomatica, Canny algorithm (Marghany and Hashim, 2010) and Matlab (Rahnama and Gloaguen, 2014). Application of filters (directional, laplacian, sobel, prewitt kernels) on particular bands or RGB combinations has been explored (Abdullah *et al*., 2013; Argialas *et al*., 2003).

When studying the shape of the earth surface in connection with the rock layers and their deformation by tectonic forces, we often notice a correlation between shapes and structures at the surface and in the subsurface according to (Short and Blair 1986). This opens the opportunity to map the characteristics of the surface and infer characteristics of the subsurface. We can describe the surface by its shape and by its structure. The surface shape depends on topography, terrain gradient and surface lithology, which we call geomorphological properties. The surface structure is determined by lithological boundaries and fracture zones outcropping at the surface, which we call litho-structural properties. Fracture zones can also be inferred from the characteristics of recent or paleo-drainage (Short and Blair 1986). Geomorphology and litho-structure allow building a static geological model. If information is available about the elevation change with time, then the statics model can be expanded into a dynamic geological model.

1.2 Problem of Statement

Since Remote sensing and geographic information system is acquiring information without any physical contact and analyzing gathered data to provide meaning full scene using human skill with the aid of device called computer and different softwares.

Ethiopian borders, desert and semi desert areas, the local geology is still unstudied at large scale due to many challenging factors such as economy, climate of area, inaccessibility of area and security problems; especially the later two factors are very common in Afar and Somali Regional states. So, this research is designed to study and provide up to date and qualified geosciences information for the country's development by assessing the areas which are more challenged, through remote

sensing and Geographic Information System method and techniques in Afar Region, Serdo area Ethiopia.

1.3 Previous Works

1.3.1 Regional Geology

Divergent plate boundaries provide the most suitable site to study how extension occurs in the Earth's crust, including the development of a rift zone and its relationships with volcanic activity. Investigations in Iceland and along submerged oceanic ridges have revealed how extension and volcanism may occur along oceanic divergent boundaries (Gudmundsson, 1995, 1998; Macdonald, 1998). On continents, the most suitable place to investigate divergent plate boundaries is the East African Rift System. In a very similar fashion to oceanic boundaries, this continental rift consists of spaced spreading segments associated with volcanism and tectonic activity (Mohr and Wood, 1976; Ebinger and Casey, 2001). The composition of volcanism varies, from basaltic to rhyolitic, as a function of the crustal thickness (Lahitte *et al*., 2003a). Nevertheless, the overall deformation pattern, characterized by large extension fractures and open normal faults with tilted hanging-walls, is remarkably similar to that observed along oceanic boundaries (Kazmin and Bacon, 2000; Le Gall *et al*., 2000; Acocella *et al*., 2003; Williams *et al*., 2004)..The Main Ethiopian Rift (MER) and Afar Rift represent the northernmost part of the East African Rift. Volcanic activity in Ethiopia started about 30 million years ago with uplift followed by eruption of large volumes of basalts (Mohr and Zanettin, 1988). However, activity has reduced since the Miocene times with eruptions of bimodal suite of basalts and more alkaline silicic lavas concentrated within the rift zone. More recent activity in the axis of the rift consisted of rhyolite volcanoes and domes as well as ignimbrites and nonconsolidated pyroclastics.The Main Ethiopian Rift is a 60–100 km wide depression with an overall northeasterly orientation. Although the average elevation of the plateau on both sides of the rift is 2300 m, the mean elevation within the rift floor is 1250 m. Two distinct fault systems are recognizable in the Main Ethiopian Rift. The older includes Miocene, north-northeast-to northeast-trending, steep, segmented, rift bounding fault systems (Wolde Gabriel *et al*., 1990; Ebinger *et al*., 1993). The younger includes Quaternary, northeast-trending faults and aligned eruptive centers affecting the rift floor (Meyer *et al*., 1975, Mohr and Woods, 1976, Boccaletti *et al*., 1998, 1999). The latter is referred to as the Wonji fault belt. The rift

valleys are a system of normal faults bordering a 40-60 km wide trough, funneling out toward north in the Afar region. In Djibouti and Ethiopia volcanic and rifting episodes are known to occur, involving magmatism and widening of discrete volcanic systems. The last occurred in 1978 (Ardukoba) and 2005 to 2008 (Dabbahu) (Ebinger, C., *et al*., 2010).Recurrence times are unknown. Those are controlled by the rifting process: stress builds up for a long period of time (century) to breaking limit. Overstretched zone of weakness opens up along pre existing faults and basalt intrudes into them at depth (dyking). Fissure eruptions may occur depending of magma supply. The caldera (central) volcanoes of the rift are underlain by crustal magma chambers during some stages of their active periods. They erupt silicic magma when overpressure breaks their roof-either as large volume pyroclastics or smaller volume domes and flows. A variety of central volcanic activity is long lasting eruptions or lava lake activity of basaltic lava at their central crater. According to Ebinger, C., *et al*.,(2010),Spreading slows down from north to south from 2.6 cm/yr in the Red Sea to about 1 cm/yr in Afar to 0.7 cm/yr in the Ethiopian Rift and 0.5mm/yr combined in the Western and Eastern Rifts across the Kenya Dome and gradually decreasing from there to the south.

1.3.2 Local Geology

Afar rift is the most active segment of the entire East African Rift System (EARS) with Erta Ale volcano being presently active. Studies by Mohr (1972) indicate that over 90% of the eruptives are of silicic composition. The Afar rift floor is dotted with a large number of rhyolitic volcanoes in the south and more basaltic centers in the north. The surface geology in the south is similar to that of the MER where ignimbrites are abundant while in the north basalt sheets of Quaternary age dominate. The volcanics overlie older sedimentary rocks in the Afar rift zone. The Afar depression of Ethiopia is a significant area of graben fracturing showing all tectonic and volcanic consequences. It is a part of the afro-Arabian rift system which extends 6500 km from the Jordon to Dead Sea rift through the red sea, the Gulf of Aden and the east African rift according to (Tazieff and Varet, 1972).

Roughly triangular shape of the Afar rift is situated where three important tectonic structures, the red sea, the Gulf of Aden and the east Africa rift system comes together in a triple junction. The types of the tectonic in the Afar region depend on the

attenuation (decreasing the thickness) of the crust through tensional movements. The tectonic movements where combined with, or followed by strong volcanic activities. In any case, tectonics and volcanism show close associations in the afar. Subsequently, tectonism and associated volcanism came into being and where in the special case of the Afar influenced and complicated by the joining of the three significant and distinct tectonic structures. According to Mohr *et al.* (1972) the faulting in the Afar shows synthetic and a synthetic fracture of tensional type with few strikes slip faulting at some localities. The existence of transform faults and big transcurrent faults is contested. The type of the tectonic was particularly described by Mohr *et al.* (1972).The origins of the brittle structures in the study area have been related with the relatively younger evolution of two dissimilar rift zones according to (Corti *et al*.2013). In the southern part of the study area predominantly exhibit N-S to NE-SW trending faults and shear joints associated with NNE-SSW trending Main Ethiopian Rift System (Fig.1.1).Fault lineation are seen plunging under steep to moderate angles to the NNE to WNW.

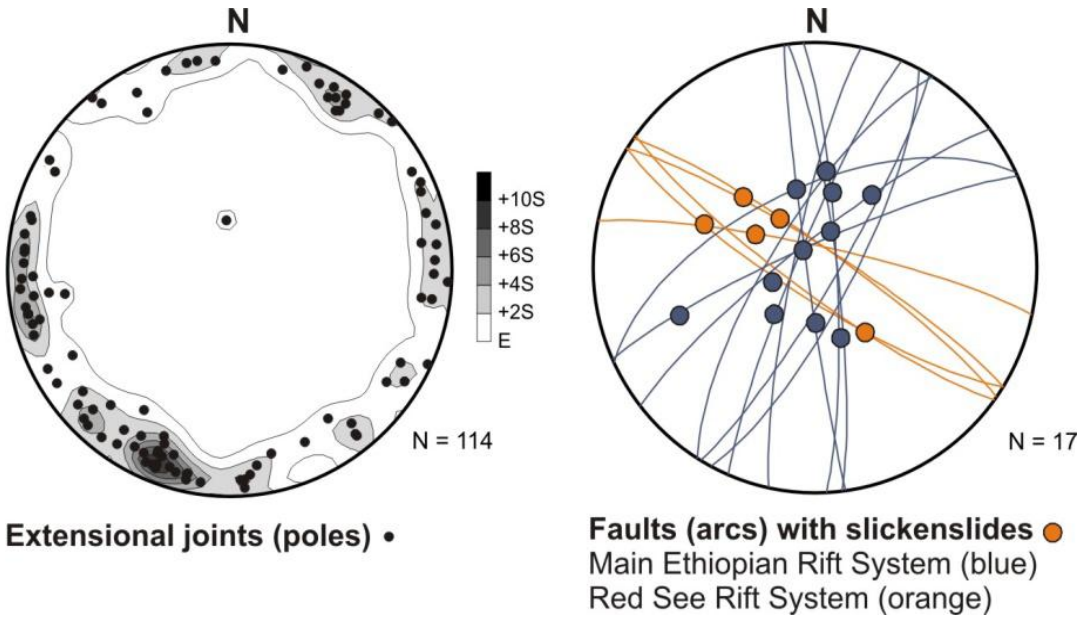

Figure 1.1 Orientation diagrams of brittle structure Poles of extensional joints**,** adopted from (Corti *et al*.2013).(on the left) and normal faults or fault zones (two different systems) with slickenslides (on the right), Projection to lower hemisphere.

During the evolution of the Afar periods of stronger and weaker tectonic and volcanic activities had been occurred. However, there have also been periods of no volcanic and tectonic activities for which Afar did not have an evolution of uniform continuity but rather have showed increased tectonic and volcanic

activities. According to (Mohr and Wood, 1976; Ebinger and Casey, 2001), the tectonic evolution of Afar shows the following activities:

- A continuous faulting during the deposition of the volcanic units over lacustrine sediments
- Period of tectonisim and volcanism
- Deposition of sediments in grabens

1.4 Research Objective

1.4.1 General Objective

The general objective of this research was mapping lithology and structures using remote sensing and GIS techniques in Serdo area, Afar Region, Ethiopian rift valley.

1.4.2 The Specific Objectives

- To identify and map the lithology and structures formed in Serdo area by remote sensing and GIS techniques and methods at 1:100,000 scale.
- Predicting the tectonic evolution of the area, and economically important resources available in that area which includes; mineral deposits and geothermal energy.
- To develop a static geological model commonly used for managing natural resources and natural hazards and quantifying geological processes in the study area
- To produce a system which minimize risk and safe energy and resource which is lost during field work in geological investigation especially in desert and inaccessible area.

1.5 Significance and Application of the Research Result

After the compilation of the study the following applicable result were generated,

- The study enhanced the understanding of the lithologic type, structures and tectonic evolution of study area and its economic contribution.
- The study provided some geosciences dataset and information to the ongoing worldwide study of geologic formation.

1.6 Scope of the Research

- Due to security problem (since the area is in national boarder), harsh climate condition and inaccessibility of the study area the cross checking /correlation of satellite result and field traverse was not completed.
- In structures investigation, it is impossible to know the exact measurement of planar and linear feature of structures (example dip angle).
- In this work by remote sensing techniques it is impossible to determine the absolute age of geological units, rocks age, dyke age, fossil age absolutely but, in some extent only the relative age is determined.

1.7 Thesis organization

This thesis has six chapters. The first chapter contains introduction, previous works, statement of the problem, objectives of research and scope of the study. The second chapter focuses on literature review on Applications of remote sensing in Geology. The third chapter is on the details of the study area and addresses resource required and the methodology followed. The fourth chapter is on results and the fifth chapter is discussion. The sixth chapter provides conclusion and recommendation based on results and discussions presented.

CHAPTER II

LITERATURE REVIEW

2.1 Remote Sensing and Geology

Remote Sensing is the science and art of obtaining information about an object, or phenomenon through the analysis of data acquired by a device that are not in contact with the object, area or phenomenon under investigation (Lillesand *et al.*, 2004).

Several important innovations in remote sensing were made in the first half of the twenty century. The most important developments to the geologist were systematic images of the Earth's surface by the three Landsat satellites. During the last few years, the role of remote sensing has been examined and utilized widely as an aid in mineral exploration.The use of multispectral remote sensing data and many ways of digital image enhancements techniques offer information so important in detecting the subtle features related to lithological variation and is therefore significant to facilitate and to confirm the field geological data acquisition and interpretation.

Many studies have shown that maps produced from remotely sensed images can serve as adequate reconnaissance geological maps for mineral resource mapping (Rajesh, 2004).

Further many studies have also shown that remotely sensed data could be employed to improve the existing maps of the area that was done by field method (Rothery, 1987; Abrams *et al.*, 1988).

Many studies also note that there is a strong correlation between mineral deposits and lineaments and emphasized the importance of lineament interpretation and analysis in localizing mineral deposits according to (Liu *et al.*, 2000 and Rein and Kaufmann, 2003). Multispectral satellite remote sensing technology provides a relatively efficient and low cost method for the geological mapping of terrains that are geologically complex or poorly or expensively accessible. Remote sensing data, such as aerial photographs and multispectral imagery data can provide more continuous and detailed information and quantitative interpretations can be made for large areas, thus enabling even the most inaccessible terrain to be mapped. However, the results of a digital

image processing and analysis require a field investigation in some selected testing areas in order to estimate the accuracy of the geological interpretation. Remote sensing has been effectively used for broad lithological mapping primarily based on principle and techniques of photo interpretation.

Faults, fractures and contacts often provide a conduit for depositional environment for hydrothermal or magmatic fluids in regions of known mineralization, and thus make excellent target for further investigation. Landsat ETM has been used to map large scale lithological information in different parts of world according to (Rencz *et al*., 1996). With the advancement in sensor technology, new sensors with better spectral resolution like ASTER (12 channels covering visible, SWIR and TIR), Hyperion (242 channels covering visible and SWIR) are being used for lithologic mapping. A significant increase in the spectral resolution has led to increase in narrow spectral band to generate hyper spectral image .The narrow spectral channels of an imaging spectrometer forms continuous reflectance spectrum of the earth surface in comparison to the narrow channels of multi-spectral.

Airborne satellite hyperspectral data has been used for mapping mineral abundancy by various researchers (Boardman *et al*., 1994; Kruse *et al*., 2003; Vinod, 2006). This technique is rapidly gaining importance for lithological discrimination. Satellite based remote sensing approach is best suited for geomorphological mapping.

Jones (1986) demonstrated the applicability of suitably processed TM imagery for geomorphologic investigation in arid and semi arid environments. Updating of geomorphological maps is great importance for environmental monitoring and sustainable development.

2.2 Utility of Digital Image Processing of Multispectral Medium Resolution Data to Geology Applications

According to Kruse, (1998) the use of enhanced images, integration of GIS and remote sensing data, and use of narrower spectral band width data has aided geological mapping, an application where the mineralogy, weathering characteristics and geochemical signatures are useful in determining the nature of rock units, the success of a classification relies on the separebility of training data into the various target classes. Thus multispectral and hyperspectral data allowing individual rock type

to be studied spectrally and signature or spectral index be obtained have greatly boosted geological investigation. Such studies have explored the utility of band ratios using Landsat and ASTER data owing their availability. According to (Boettinger *et al*., 2008; Campbell, 2002, 2009; Chen and Campagna, 2009) landsat bands are known for particular applications: band 7 (geology band), band 5 (soil and rock discrimination) and band 3 (discrimination of soil from vegetation)). Band ratios are also known for eliminating shadowing and topographic effects and therefore suit for complex terrain. The need to normalize band ratios to ease scaling, has paved way for spectral indices while still maximizing the sensitivity of the target features. Examples of band ratios that have been used in geology applications using Landsat are: 3/1-iron oxide (Gad and Kusky, 2006), 5/1- magnetite content (Sabins, 1999), 5/7-hydroxyl bearing rock (Sultan *et al*., 1987), 7/4 - clay minerals (Laake, 2011), 5/4*3/4-metavolcanics (Rajendran *et al*., 2007).

Other band ratios possible with ASTER data and hyperspectral data are discussed by (Ninomiya *et al*., 2005).

RGB combinations are image enhancement techniques which provide powerful means to visually interpret a multispectral image and they can be real or false color composite (FCC) utilizing individual bands or band ratios. In these respect, band ratios, band or principal component (PC) combinations have been explored as a means to distinguish lithology. Examples using band ratios are: Kaufmann ratio (7/4, 4/3, 5/7), Chica-Olma ratio (5/7, 5/4, 3/1) using Landsat bands (Mia and Fujimitsu, 2012), Sabin's ratio (5/7, 3/1,3/5) (Sabins, 1997), while Abdeen *et al*., (2001) investigated ASTER band ratio combinations in mapping geology for arid regions and concluded that the ratios (4/7, 4/1, 2/3*4/3) and (4/7, 4/3, 2/1) were equivalent to Landsat Sultan (5/7,5/1, 5/4*3/4) and Abrams (5/7, 3/1, 4/5) combinations respectively. Similarly using band combinations, ASTER combination (7, 3, and 1) was found to be the equivalent of Landsat (7, 4, and 2).

CHAPTER III

MATERIALS AND METHODS

3.1 Description of the Study Area

The study area lies in Afar National Regional State in zone 1 at ~700 km from Addis Ababa to Djibouti cross country road in north east of Ethiopia. The study area is lying in subtropical climate classified as semi-arid and arid climate zones. The temperature ranges from 26ºC to 36ºC. The temperature commences to increase from April and reaching up to 42ºC in June and July. Rainfall is bi-modal throughout the region with a mean annual rainfall below 500 mm in the semi-arid decreasing to 150 mm in the arid zones. The region receives rain from (June to September) and two short rainy months December and March to April. The area is characterized as desert scrubland. Vegetations are mostly drought resistant plants such as small trees, shrubs, and grasses. The geographic location of the study area bounded by latitude 11^{o} $00'00^{"}$N-12^{o} $00^{'}$ $00^{"}$ N and longitude 41^{o} $00^{'}$ $00^{"}$E-42^{o} $00^{'}$ $0^{"}$ E covering a total area of 12321 km^{2} (Fig. 3.1).

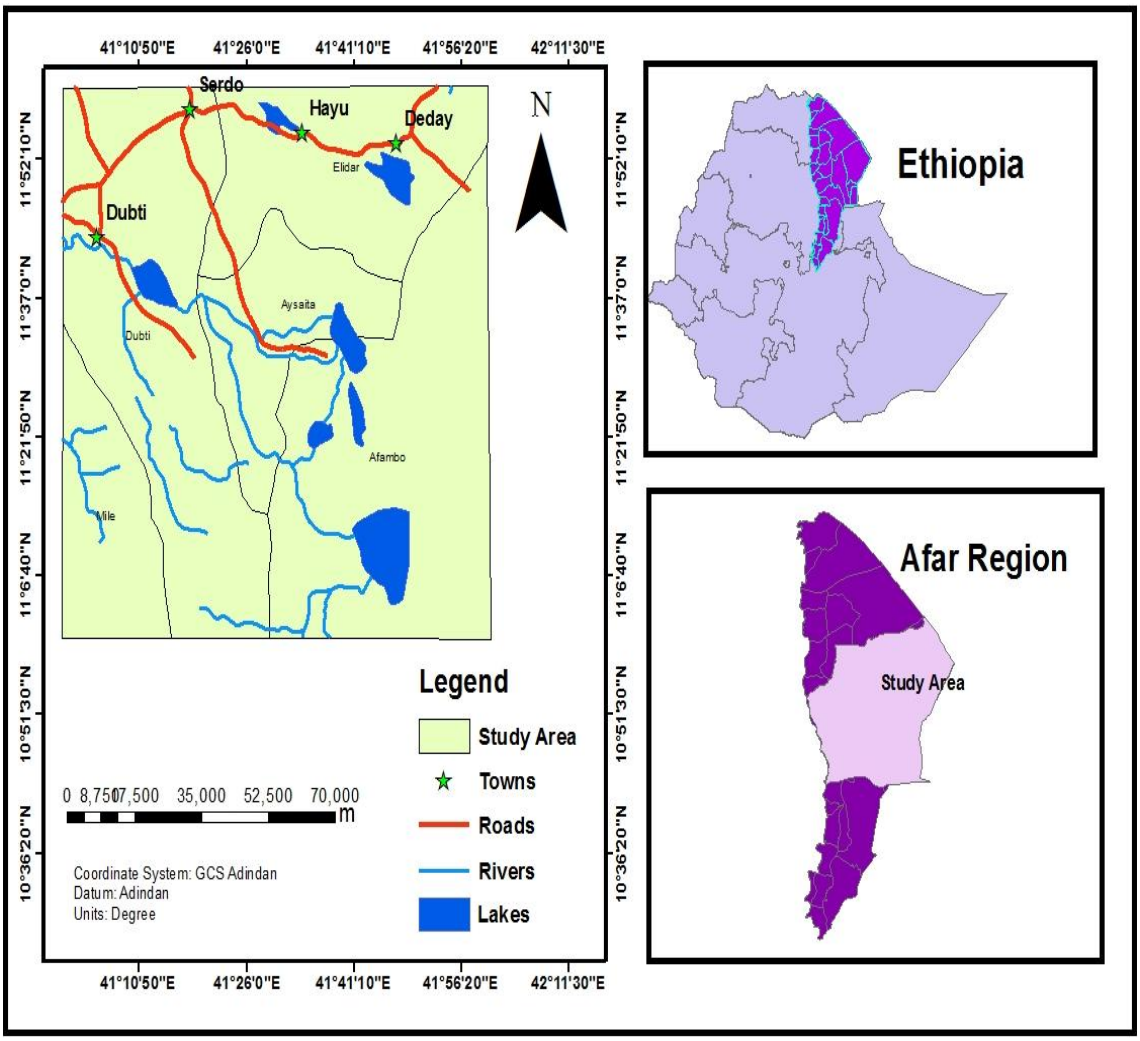

Figure 3.1 Location map of the study area.

3. 2 Physiography of Area

Serdo area is a part of the eastern Afar depression. Physiographic regions in the area found enclosed with an elevation ranging from 100 m (graben) and 1400 m above sea level. Graben and horst physiographic regions are found alternatively covering large areas showing in the 3D surface of the study area (Fig 3.2).

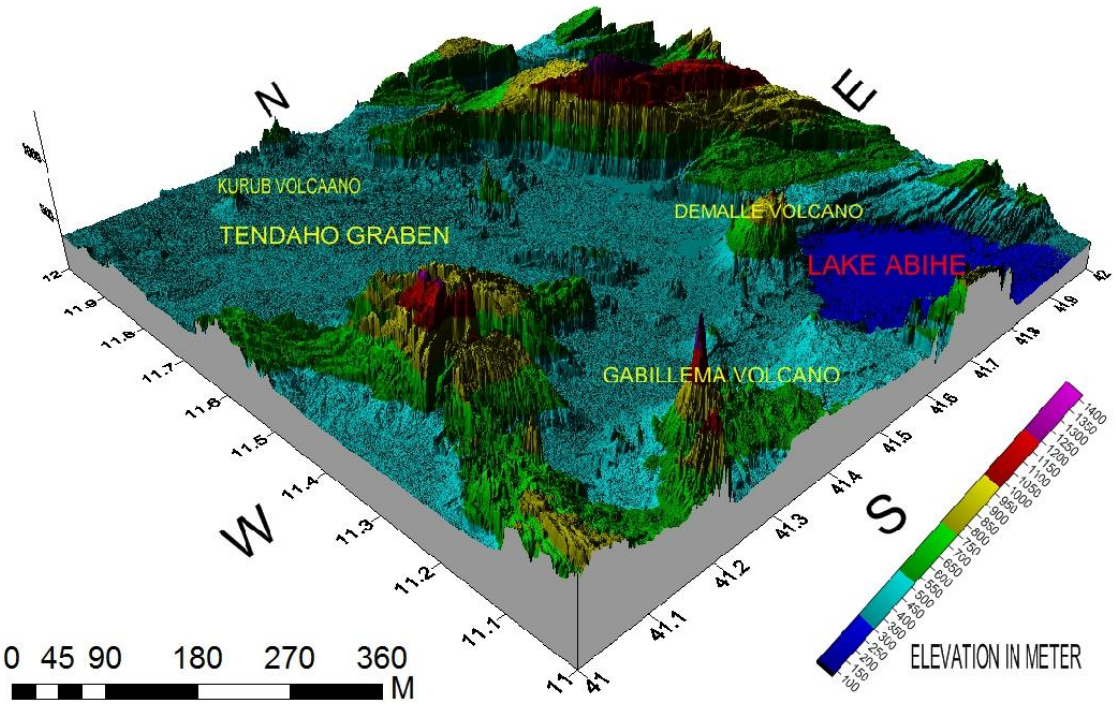

Figure 3.2 Topography of study area generated from 30 m resolution DEM.

North-south and east-west topographic profile of the study area shows that the area is highly undulated and characterized by many cliffs and escarpments (Fig 3.3) shows the topographic profile of study area.

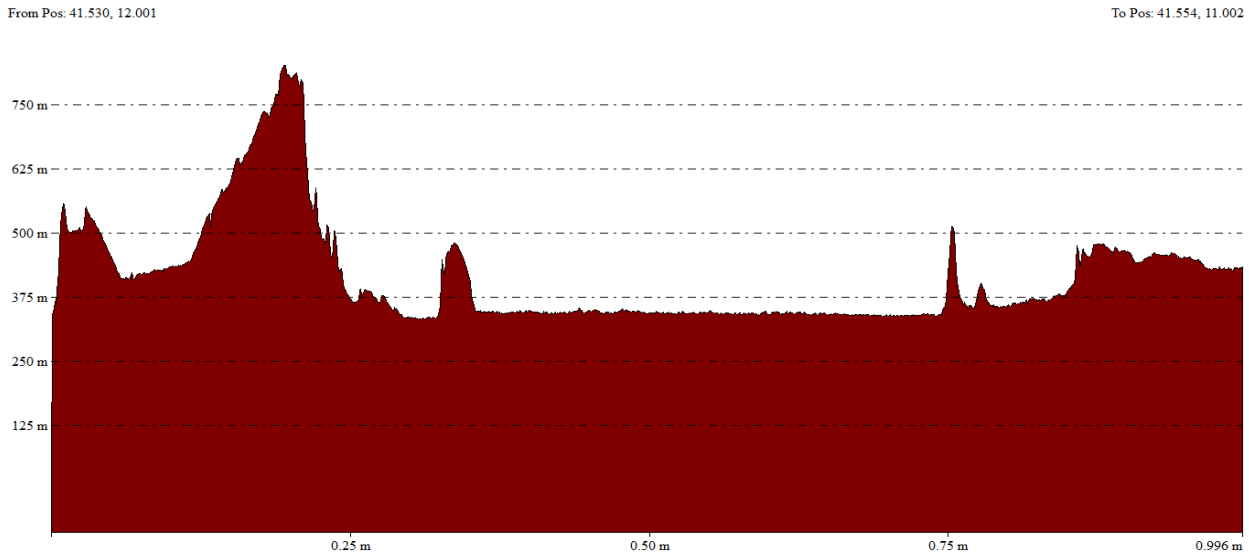

(a)

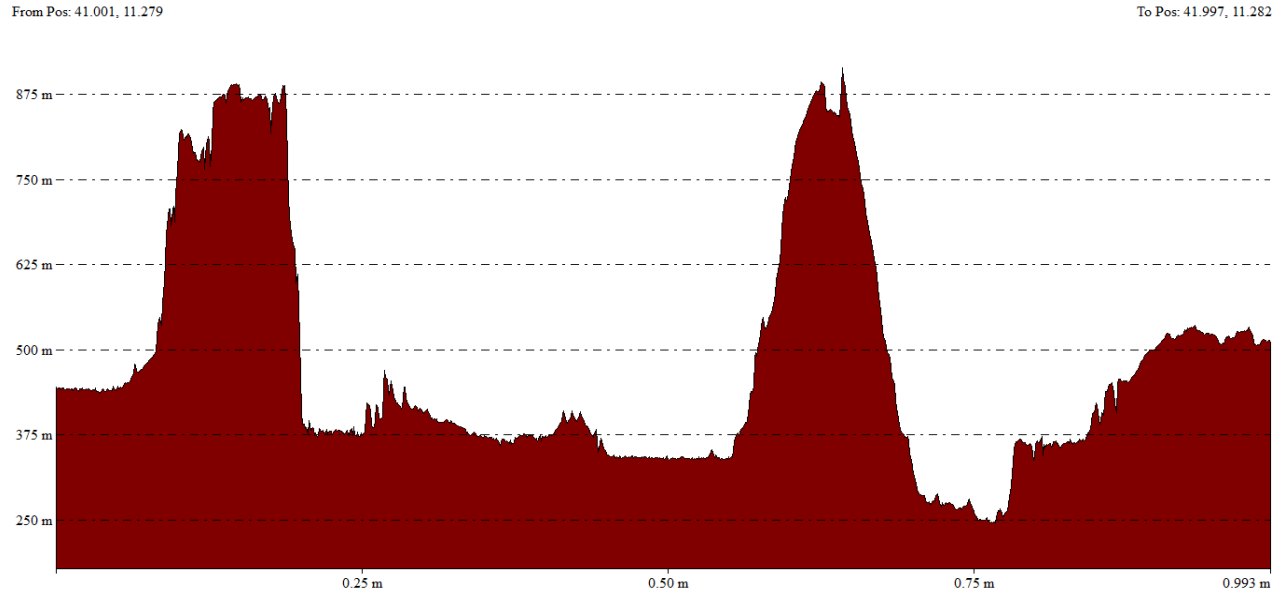

(b)

Figure 3.3 Topographic profile of study area. (a) north-south, (b) west-east generated from 30 m resolution DEM.

3.3 Materials

3.3.1 Data and Software

Primary task of the present study encompassed gathering of relevant and available data that are essential to accomplish the study objectives, accordingly the following study materials were important for research work.

Earth observation satellites map the physical properties of the earth surface and near-surface. In the context of geological mapping we distinguish two types of electro-magnetic methods.

Passive optical methods: use the sunlight as the source and measure the reflectance of the earth surface in the visible and infrared spectral bands. The cloud-free level 1T (terrain corrected) Landsat 8 image of 2015 from U.S Geological Survey data set were used in this study.

Active microwave radar methods: use a microwave source onboard of the satellite and measure the back-scatter from the earth. Digital elevation model, DEM 30 m from the Shuttle Radar Topographic Mission (SRTM) data were used in this study.

Landsat 8 satellite image from U.S Geological Survey data set, digital elevation model DEM (Shuttle Radar Topography Mission SRTM) 30 m from U.S Geological Survey data set to provides terrain relief and facilitate identification of geological structures, existing published geological map covering the research study area (1:250,000) from Ethiopian Geological Survey, published topographic map covering the research study area (1:50,000) from Ethiopian Mapping Agency this forms the geographic base map of the area and is essential for geo-referencing, , measuring tape (meter),compass ,geologic hammer ,sample bag, digital camera, GPS (global positioning system) laptop (preferable), softwares such as Microsoft Office2007, ERDAS Imagine 2014, ArcGIS10, Surfer11(for contouring, gridding and 3D surface mapping) and Global mapper.

3.4 Methodology

The methodology involved the collection of primary data which includes spatial data such as landsat 8 satellite image, DEM data and non-spatial data such as field data, different map sheets, and measurements surface rendered attributes DEM data 3Dmodel, hills hade, surface derived attributes slope, aspect, curvature from secondary data previous works and reports. After data collection, image preprocessing techniques applied, data analysis and synthesis (False color composite (FCC), True color composite (TCC), convolution, principal component analysis (PCA) and intensity hue saturation transformation(IHS), then a field investigation in some selected test areas in order to validate the accuracy of the visual interpretation. The detailed framework of the study was presented in (Fig.3.4).

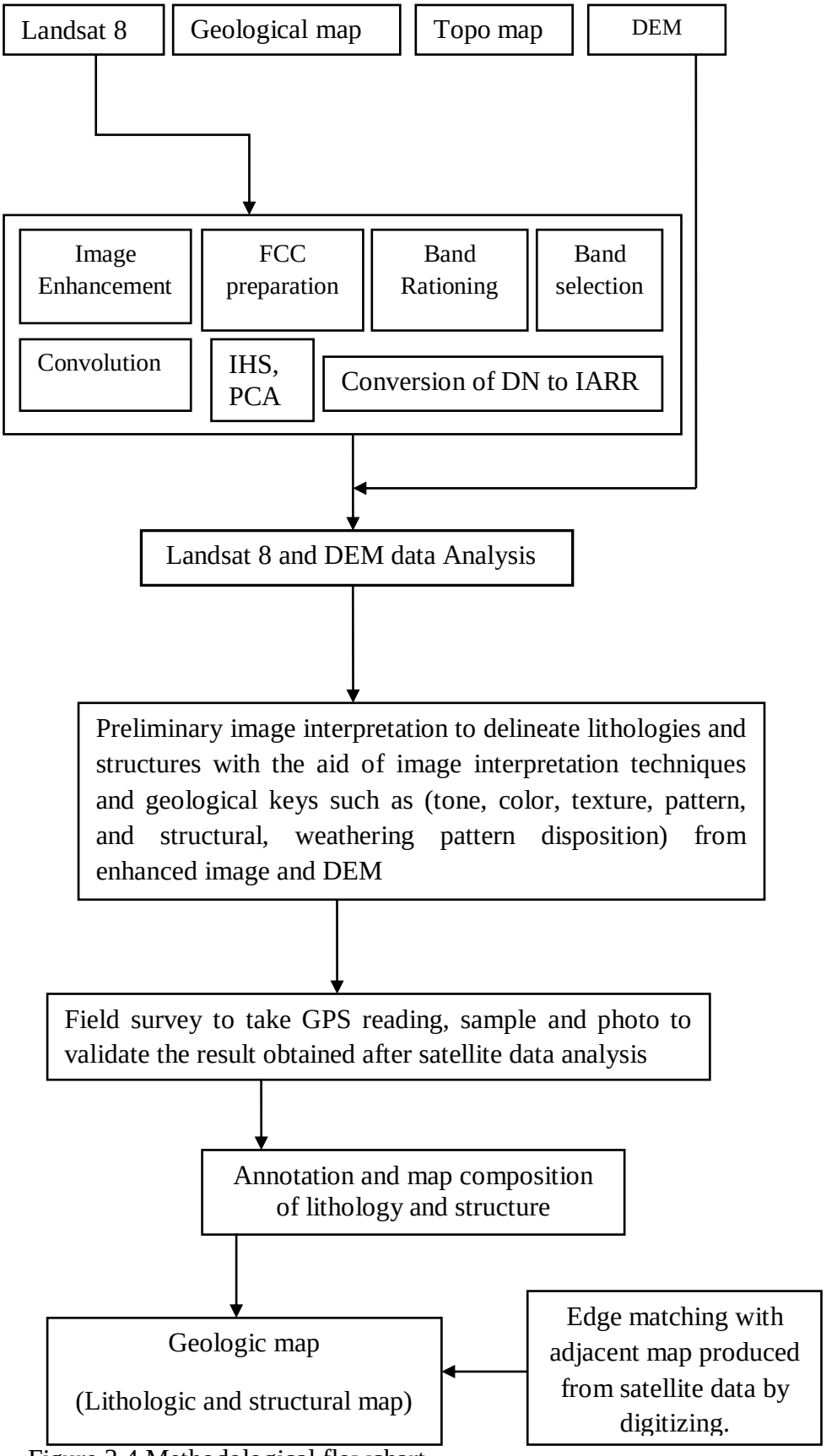

Figure 3.4 Methodological flowchart

To achieve the general and specific objectives, the following methods and approaches has been followed.

3.4.1 Pre-Field Work

The activities that are conducted during pre- field work were:

Relevant data such as topographic map and geological map were collected and analyzed, the, project area from topographic map was delineated.

Shuttle radar topographic mission DEM data and landsat8 satellite images of Entity ID: LC81670522015206LGN00 Coordinates: 11.56789, 41.42345 Acquisition Date: 25-JUL-15

Path: 167

Row: 052 were downloaded and preprocessed.

The major geological structures and lithological contacts based on the DEM data from preprocessed SRTM, and satellite image of landsat 8 were identified and located visually.

3.4.2 Data Preparation and Analysis

3.4.2.1 Applications of Geographic Information System

In this study GIS was primarily applied for the purpose of data integration, visualization, and cartographic work and for data analysis.

3.4.3 Processing of Landsat 8 OLI/ TIRS Data

Landsat 8 data were converted to surface reflectance using the Internal Average Relative Reflectance according to (IARR) method (Ben-Dor *et al*., 1994). Ben-Dor *et al*. (1994) recommended IARR reflectance technique for mineralogical mapping as a preferred calibration technique, which does not require the prior knowledge of samples collected from the field. During the atmospheric correction, raw radiance data from imaging spectrometer is re-scaled to reflectance data. Therefore; all spectral

are shifted to nearly the same albedo. The resultant spectral can be compared with the reflectance spectral of the laboratory or filed spectra, directly.

The full subset Landsat 8 bands were imported in geographic coordinate system. The imported images were path oriented. In order to transform the to north-up UTM, the images were re-projected using the following parameters: UTM Projection; Adindan UTM zone 37N and Nearest Neighbor re-sampling method. The study area lies on Grid UTM zone 37.The landsat 8 spectral subset bands have deferent spatial resolutions. The coastal/aerosol, visible and near infrared (VNIR), SWIR-1 SWIR-2, bands 1, 2, 3,4,5,6 and 7 are 30 m resolution. The thermal inferred (TIR-1, TIR-2) band 10 and 11are provides in 100m resolution, Cirrus band (9) 30 m and Pan band (8)15 m. The Visible, NIR and SWIR bands are merged to panchromatic 15 m resolution to attain a consistent resolution for subsequent processing. The panchromatic and cirrus cloud (band 9) bands and thermal inferred (TIR-1) band 10 are supplementary tools in this study (Table 3.1) shows Landsat 8 OLI and TIRS Bands characteristics.

Table 3.1 Landsat 8 OLI and TIRS Bands characteristics.

Spatial resolutions and subsystems	Spectral range(μm)	Bands
30 m Coastal/Aerosol	0.435−0.451	Band 1
30 m Blue	0.452−0.512	Band 2
30 m Green	0.533−0.590	Band 3
30 m Red	0.636−0.673	Band 4
30 m NIR	0.851−0.879	Band 5
30 m SWIR-1	.566−1.651	Band 6
100 m TIR-1	10.60−11.19	Band 10
100 m TIR-2	11.50−12.51	Band 11
30 m SWIR-2	2.107−2.294	Band 7
15 m Pan	0.503−0.676	Band 8
30 m Cirrus	1.363−1.384	Band 9

3.4.3.1 Band Selection

For the purpose of image display only three bands or band combinations, each directed to one of the primary color-gun (Red, Green and Blue), are required. In order to enhance a desired target and avoiding the redundancy of information spectral bands having the most information contents should be selected. Different workers demonstrate the possibility to select band combinations that contains the highest possible amount of information using statistical approach. In this study, the optimum index factor (OIF) method introduced by Chavez *et al*., (1982) was adapted. The Optimum Index Factor (OIF) is a statistical calculation of every possible 3 band combination, based on total variance within bands and correlation coefficient between bands.

The index given by:

$$OIF = \sum_{i=1}^{3} SDi \,/\, \sum_{i=1}^{3} ABC(CCj) \qquad \text{eq (1)}$$

Where SDi is the standard deviation of band i and ABC (CC j) is the correlation coefficient between any two of the possible three pairs. The highest value of OIF should be the three bands having the most information content (Chavez *et al.*,(1982).

Various band combinations were visually inspected to support the statistical method, and most of the high rank band combinations give helpful geological information. The band combination 7, 4 and 3 with the lowest OIF at rank number of higher values provides good color contrast between different lithologic units and structures also apparently enhanced (band 5.4 and 3) for landsat 8 in this work.

3.4.3.2 Haze Correction

Space born optical sensors recording data in the visible and shortwave inferred spectrum receive solar radiation reflected from the Earth's surface and radiation scattered by the atmosphere. Since the atmospheric effect due to haze, aerosol, and etc. modifies the radiation reflected at the ground reducing image contrast, and contributes an additive term, correction is necessary in order to convert the "at sensor" or "top-of-atmosphere" radiance to ground leaving radiance. To determine the portion of the at-sensor or radiance that is attributable to ground properties, while subtracting out the portion that is attributable to atmospheric effects in the situation when actual

atmospheric data are not available is done by “dark object subtraction” approach given by (Crane, 1971). The method is based on the assumption that the atmospheric scattering throughout the scene is uniform and somewhere in the image there is a pixel with zero reflectance, such that the radiometric contribution from this pixel represent only the additive term.

3.4.3.3 Image Enhancements

Landsat 8 data was digitally processed and several spatial and spectral enhancement techniques namely: contrast stretching, HIS transformation, principal component analysis (PCA), band rationing and spatial filtering were applied. The enhancement gave substantial results in geological interpretation is briefly summarized in the following section.

3.4.3.4 Linear Contrast Enhancement

Contrast enhancement is one of the most widely used image processing techniques for geological studies. It is the process of redistributing the brightness levels in an image to utilize the entire dynamic range of the display device. In order to produce an enhanced image during data processing the raw data stretch over the quantized range of grey value (256 for 16 bit data). The resulting enhancement, however, is strongly controlled by mean and standard deviation statistics of the input data and consequently influences the resulting color in image composites since they regulate the brightness of the bands under consideration and thus the corresponding colors.

For this study the stretched images have been interpreted for lithologic and structures interpretation.

3.4.3.5 Intensity Hue Saturation Transformation

According to (Sabins,1987) Intensity Hue Saturation (IHS) transformation is a process in which a bands Red Green Blue composite is decomposed into intensity (I), hue (H), and saturation (S) components and after manipulated then it is transformed back to the RGB space for interpretation. Intensity represents the brightness, hue signifies the dominant wave length, and saturation is related to purity of a color (Sabins, 1987). The advantage of this technique is its ability to effectively separate

intensity and spectral information from standard image, and the possibility to convert IHS elements back to RGB space. The resulting enhanced color images are easier to interpret, as the spectral information. (Hue) is not changed during transformation.

3.4.3.6 Principal Component Analysis

The principal component analysis (PCA) transformation is a multivariate statistical method used to compress multi spectral dataset into few PC images in which spectral difference between materials become apparent in PC image than individual bands (Sabins, 1987; Gillespie *et al*., 1986). Principal components are commonly calculated using the covariance matrix obtained from the input multispectral data where by the corresponding eigenmatrices is also determined. In this study, PCA was performed on landsat8 data covering the 7 bands (Visible, NIR and SWIR). For lithologic discrimination and the color composite created from the PC images gives valuable geological information.

3.4.3.7 Band Rationing

To evaluate the Landsat 8 data different Red Green Blue color combination images, band ratios were applied for enhancing the lithologic units. Band rationing is a technique where the digital number value of one band is divided by the digital number value of another band. Band ratios are very useful for highlighting certain features or materials that cannot be seen in the raw bands (Inzana *et al*., 2003, Pour *et al*., 2013, 2014).

This procedure involves the division of two bands, where the band with high reflectance features of the given material is assigned as numerator, while the other band with high absorption feature for the same material is assigned as denominator. Rationing can be thought as a method of enhancing minor difference between materials by defining the slope of the spectral curve between two bands. The resultant gray-scale band ratio image is not a direct measurement for the material's contents, rather it mark the area with highest possibilities for the presence of the given material. The combination of three-band ratio image as red-green-blue (RGB) image is useful for the interpretation of the result. Band rationing and combinations with most contrast were also investigated using Drury, (1993) principle whereby, for bands

ratios involving geology, a higher band is divided by a lower band. From algebra combinations and permutations, bands (4, 6 and7) as numerator for landsat 8.Thus combinations (4/3, 6/2, 7/3) were found to have the best contrast and they formed the input for classification.

3.4.3.8 Spatial Enhancements

One of the characteristic features of the satellite images is a parameter called spatial frequency which is defined as the number of changes in brightness value per unit distance for any particular part of an image. According to (Jensen, 1996), if there are very few changes in brightness value over a given area in an image, this is referred to as a low-frequency area. Conversely, if the brightness values change dramatically over short distance, this is an area of high frequency. Spatial filters emphasize or deemphasize image data of variable frequencies that refer to the roughness of the total variation (Lillesand, *et al*., 2004). The process involves matrix operations where the spatial distribution of the pixel and the moving window size play an influential role. Filters that operate in the frequency domain are implemented through the Fourier transformation, whereas those which operate in the spatial domain of the image itself are known as convolution filters (List, 1993).

3.4.3.9 Processing of Digital Elevation Model

Compared to two-dimensional satellite data, a Digital Elevation Model (DEM) has the advantage of representing the vertical extension of the earth's surface by assigning height values for every pixel. The use of DEM has a marked interest for geological mapping especially for highly vegetated terrains and urban areas.

A C-band system (5.6 cm wave length; C-RADAR) and an X-band system (3.1 cm wave length; X-RADAR) 30 m resolution of Shuttle Topographic Mission Radar (SRTM) are downloaded from USGS and geometric correction as well as speckle reduction (despeckle) processing applied. The operational goal of C-RADAR is to generate contiguous mapping coverage as called for by the mission objectives. X-RADAR generated data along discrete swaths 50 km wide. These swaths offered nearly continuous coverage at higher latitudes.

Several processed Digital Elevation Model (DEM) products, such as the hill- shading, painted shaded-relief, maps of slope and aspect have been processed for the identification of geological structures. In this study spatial enhancement is mainly applied to facilitate visual interpretation of image and DEM data for the purpose of structural mapping using convolution filters. For the smaller and medium size structures identification the mid-low filters of 3x3 window edge detection filters known as Gradient-Soble and Gradient-Prewitt were utilized and for the larger structures 7x7 window size directional filters were used, adapted from Kenea, (1997).

3.4.4 Field Work

Various data types are collected during field work: One field visit with a total of 15 days was conducted during 1−16 December, 2015 for verification of the preliminary interpretation results. Due to inaccessibility and hot climate of the study area, only the north and northeast parts were visited. Global positioning system (GPS), topographic maps (1:50,000 scale) digital camera and interpreted maps resulted from satellite image were used. Global position of field observation points and collected samples note on observations were recorded and summarized in (Table 3.2)

Table 3.2 Observation points and Petrographic description for collected sample.

Sample code	Easting	Northing	Sample description	Rock type
ASR-001	724710	1239845	Color- brownish to red Texture_ coarse grains Minerals-feldspars(50%),quartz and others	Ryholite
ASR-002	724380	1240520	Color- reddish Texture_ fine grains Minerals-quartz (70%), feldspars and others (30%)	Ryholite
ASR-003	711515	1294340	Color- dark gray Texture_ fine grains Minerals-olivine (80%), pyroxene and others (20%)	Basalt
ASR-004	725460	1247960	Color-reddish gray Texture-vesicular Minerals-olivine plagioclase (60%)	Vesicular Basalt
			Color-gray	

ASR-005	727490	1241782	Texture-fine to coarse grains Minerals-pyroxene, feldspar (70%)	Ryholite
ASR-006	726860	1241950	Color-reddish gray Texture-fine grains Minerals-othoclasefeldspar(65%),orthopyroxene	Ryholite
ASR-007	724950	1242030	Color-gray Texture-fine Minerals-feldspar(60%),quartz	Ryholite
ASR-008	710275	1294290	Color-gray Texture-medium grains Minerals_plagoclase(75%),olivine	Basalt
ASR-009	778420	1299330	Color-light gray Texture-fine grains Minerals – feldspar(75%),quartz	Ryholite
ASR-010	776230	1288085	Color-brownish Texture-fine grains massive volume Minerals-plagioclase(70%),olivine	Vesicular Basalt
ASR-011	771820	1290580	Color-brownish Texture-fine grains Minerals- olivine(50%) ,plagioclase	Vesicular Basalt
ASR-012	770590	1286791	Color-dark brown Texture-medium grain Minerals-feldspars(65%),quartz	Ryholite
ASR-013	788990	1281161	Color-brownish Texture-medium grain Minerals-olivine (30%), pyroxene (35%), plagioclase (35%)	Basalt
ASR-014	786480	1291295	Color-brownish Texture-fine grains Minerals-olivine (80%) and pyroxene	Vesicular Basalt
ASR-015	787470	1314540	Color-brownish Texture-fine grains Minerals- olivine(75%) and pyroxene	Aphanitic Basalt
ASR-016	785685	1315470	Color-brown and gray Texture-medium to coarse grain Minerals-plagioclase(70%),olivine, and	Basalt

			others	
SAR-017	802560	1305435	Color-brown Texture-fine grain Minerals-olivine (75%), plagioclase (25%)	Basalt
ASR-018	711060	1297050	Color-light gray to reddish Texture-coarse grain Minerals-olivine(70%),plagioclase(20%) and others	Scoriaciuos Basalt
ASR-019	807520	1303020	Color- reddish to brownish Texture- coarse grain Minerals-olivine(60%),plagioclase(30%) and others	Scoria

3.4.5 Post Field Work

- Field information was compiled in GIS software to show generated geological map, which shows lithological units, major geological features and structures.
- Finally, by integrating the pre field, during field and post-field works, a hardcopy of large scale geological map of the study area with a scale of 1:100,000 and static geological model was produced.

3.5 Image Interpretation

Visual image interpretation is carried out by geologist perception, spontaneous recognition, and logical inference (reasoning by professional knowledge) of the researcher. The interpretation of lithology and structure was performed by applying image interpretation keys, such as color (tone), texture, shapes, patterns and interrelationship between features that may have geological significance. From processed landsat 8 images, volcanic rocks such as lava, Rhyolites and vesicular basalts are clearly identified by their pattern or grey color, alluvial deposit and sediments are also clearly identified by their tonnage or brown color. Data from field visit were utilized for image interpretation and verification of results obtained from digital image processing. Enhanced true color composite image provides a good overview of the study area in color composite that is most familiar and close to natural (Fig 3.5) shows the processed landsat 8 image of the study area.

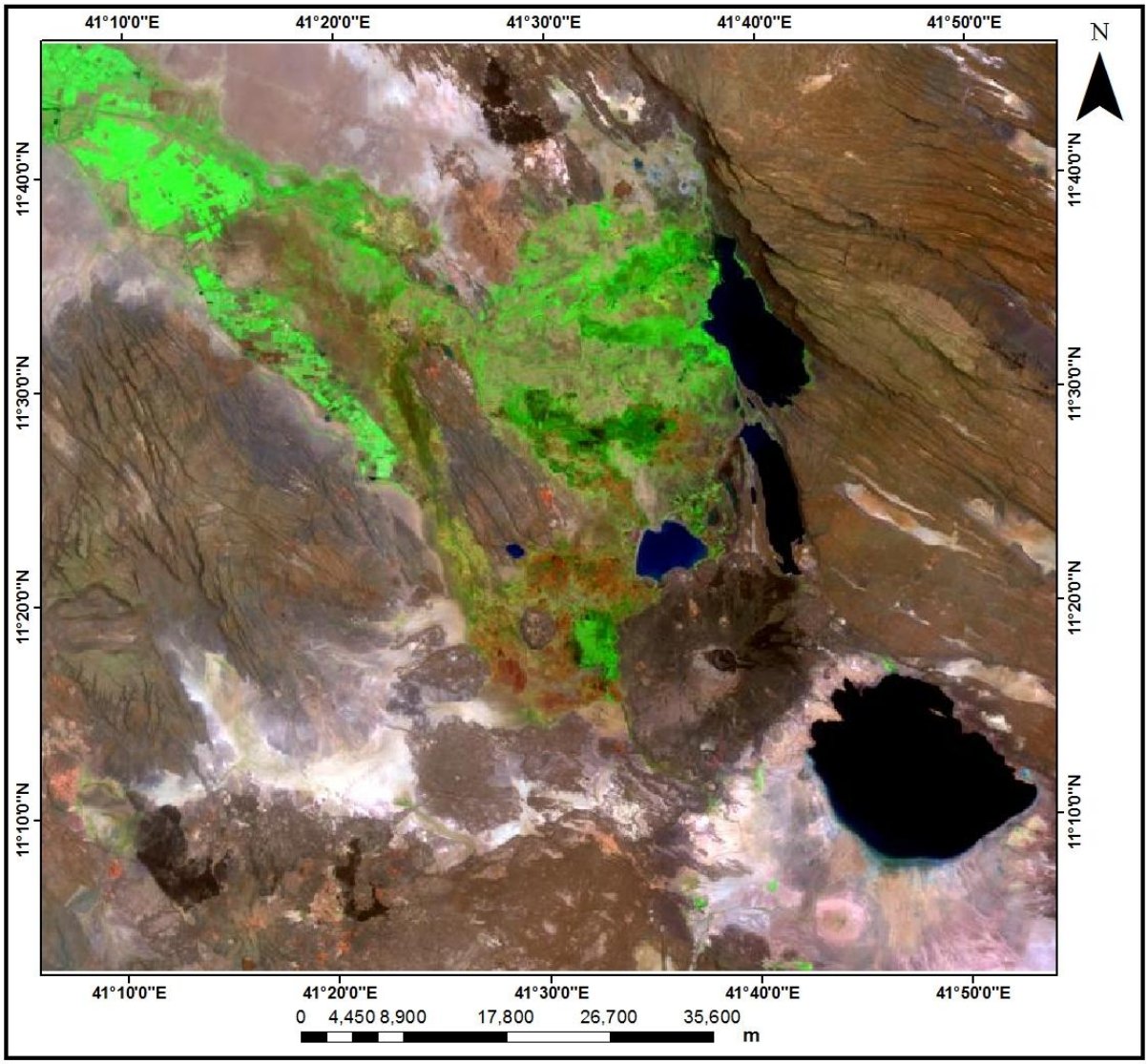

Figure 3.5 Landsat 8, True Color Composite Band combinations of RGB 7, 5, 3 of the study area.

3.6 Lineaments Interpretation

In order to understand geological significant of structures and easy of data interpretation the geological structures are grouped into parts, based on relative homogeneity of measured linear features. The presence of common regional fault and graben system has pictured the specific physiography of study area. These faults and graben systems are categorized according to their size extent.

3.6.1 The Graben Systems

3.6.1.1 The Tendaho Graben

The graben is an elongated block of earth's crust lying between two faults and displaced downwards, as in rift valley.

The Tendaho graben is one of a major structure identified in the area trending in NW direction and larger throw observed on the east bounding faults. This graben is floored by alluvial deposit, newly emerging land features and recent volcanic craters and domes. Open fissures, fractures and NW striking active normal faults were also observed at the floor of the rift, some of which were diffused into the scoria cones.

3.6.1.2 The Axial Grabens

The orientation this (around east of Gumarre lake, Dobi and Guma) grabens trend is NW and expressed as complex zone of escarpments consisting faults which seemed to be rotated. These grabens are floored by alluvial sediments and evaporate. Whereas the fault ground were covered by aphanetic and vesicular basalts. During field work attitude of bedding, fractures and dyke orientation are checked. The field observation also witnesses those major structures orientation coincides with the direction of NW faults strike.

3.6.1.3 Volcanic Calderas

These geologic features are relatively the youngest features seen in the study area from morphology structures because, they exhibit undisturbed appearance. According to visual interpretation four volcanic calderas are identified. This are Kurub volcano at the north,Demalle volcano and Gabillema volcano at the south. In addition to the above mentioned geologic features, water bodies and vegetated areas are also identified by image interpretation techniques (Fig 3.6) shows the visually interpreted major geological features in the study area.

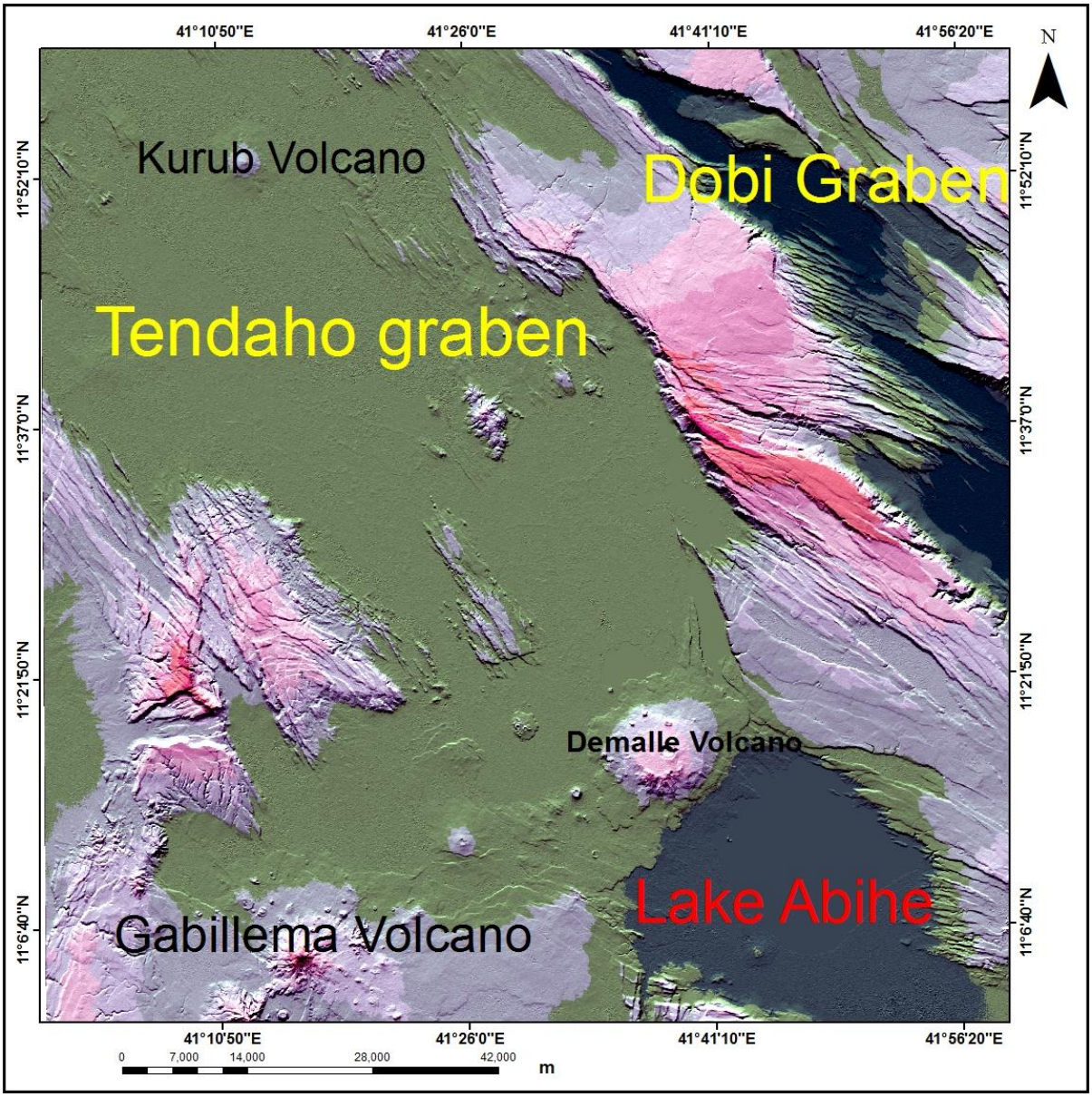

Figure 3.6 visually interpreted major geological features in the study area.

CHAPTER IV
RESULTS

4.1 Lithologic Mapping

4.1.1 Enhanced False Color Composite

Lithologic and structural information is generally well contained in many of the high ranking band combinations. Band composite, (5, 4, 3) and (7,4 ,3) in RG B contains the maximum information were given in (Fig.4.1). The contrast between the different lithologic units were also apparently enhanced in band composite7,5 and 3 in RGB ,selected by visual inspection of various band composite possible from landsat8 VNIR and SWIR data.

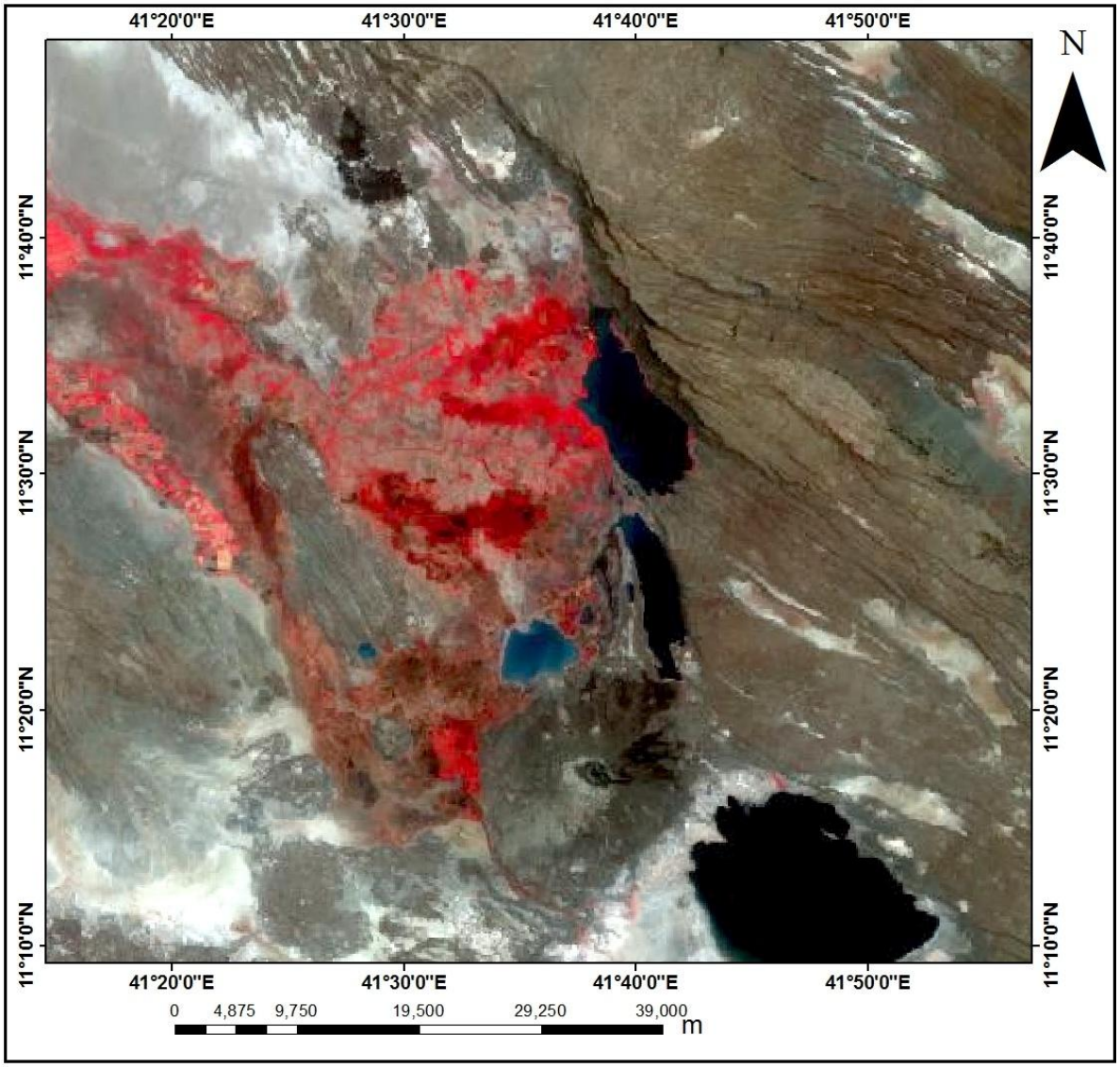

Figure 4.1 Enhanced False color composite from landsat 8 bands of (5, 4, 3) in RGB.

4.1.2 Intensity Hue Saturation Transformation

The intensity and spectral information of lithologies were effectively separated from that of standard image by intensity hue saturation transformation. Figure 4.2 shows intensity hue saturation transformed image of the study area.

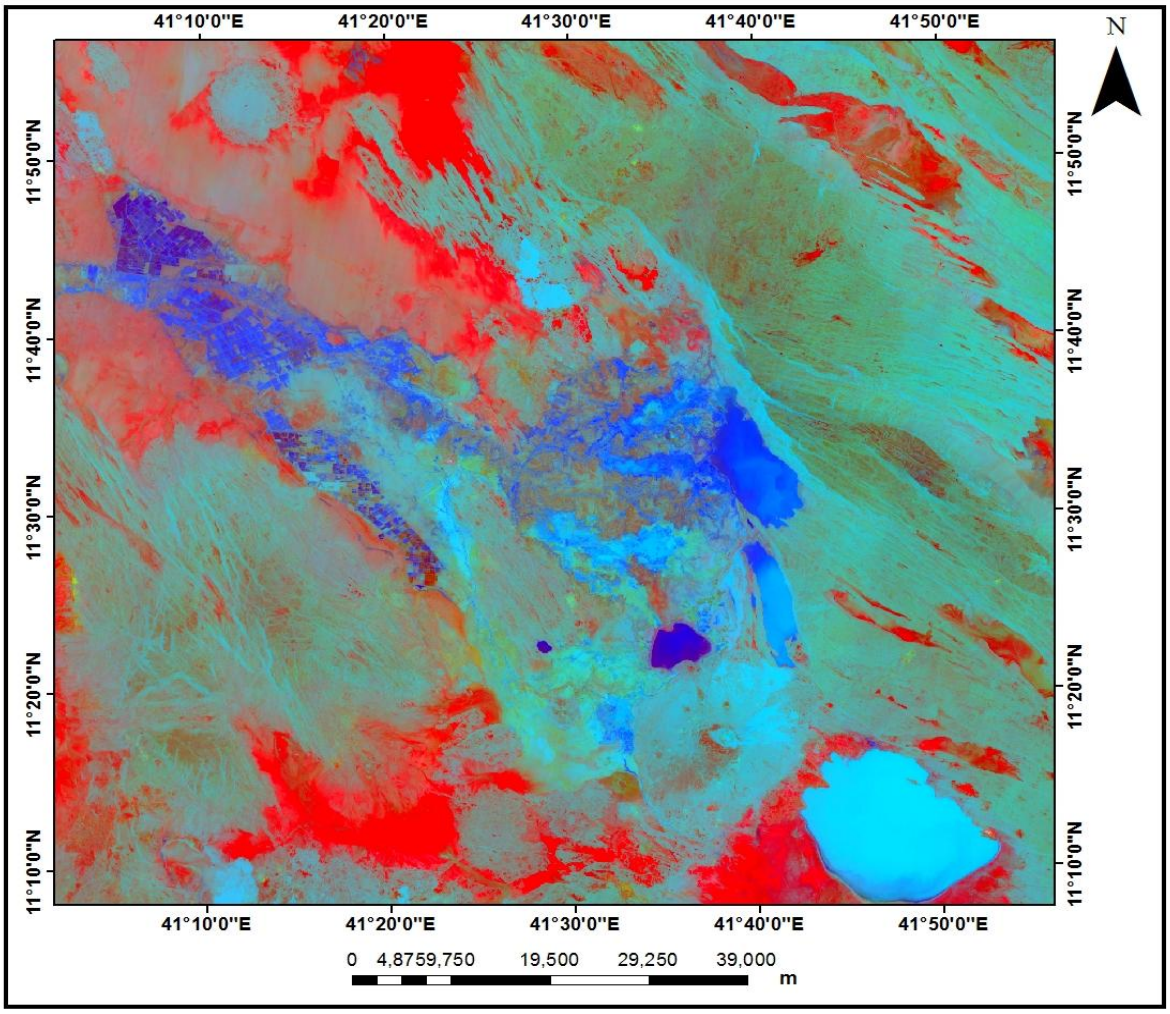

Figure 4.2 Intensity hue saturation transformed image of the study area.

4.1.3 Principal Component Analysis

PCA was performed on seven (7) bands. Compressed redundant data values into bands, which are often more interpretable than the source data were shown by PCA. This compresses multi spectral dataset into few PC images in which spectral difference between materials become apparent in PC image than individual bands.

The eigenvector and eigenvalue statistics used for the transformation of landsat 8 OLI (7 bands) was showing in Table 4.1.

Table 4.1 Eigenvector and eigenvalue statistics for landsat 8 OLI (7 bands).

Eigenvector	**PC1**	**PC2**	**PC3**	**PC4**	**PC5**	**PC6**	**PC7**
Band1	0.1556	-0.1458	0.2888	0.5145	-0.1035	-0.3492	0.6882
Band2	0.2041	-0.1762	0.3519	0.4898	-0.1335	-0.1898	0.7138
Band3	0.2882	-0.1948	0.4194	-0.0058	-0.0361	0.8279	-0.1278
Band4	0.3888	-0.3335	0.3558	0.6776	0.01827	-0.3892	-0.0040
Band5	0.4922	0.8244	0.1695	-0.0021	0.2155	-0.0533	0.0039
Band6	0.5076	-0.0144	-0.5023	0.0080	-0.6983	0.0417	-0.0151
Band7	0.4470	-0.3445	-0.4572	-0.1897	0.6600	0.0243	.0124
Eigenvalue	1759.03	1367.06	7124.2	425.4	307.58	44.40	6.44

PC1, with positive loading from all landsat 8 bands, contains significant albedo and topographic information and that accounts for high correlation between the input bands. PC1, PC3, PC4 and PC5 display fair lithologic contrast and the rest of the PC (PC2, PC5, and PC7) show noisy images and appear to be less informative. RGB composite of PC1, PC3 and PC4 have better color contrast and allowed best lithologic discrimination. Figure 4.3 showing the landsat 8 PC1 image of the study area.

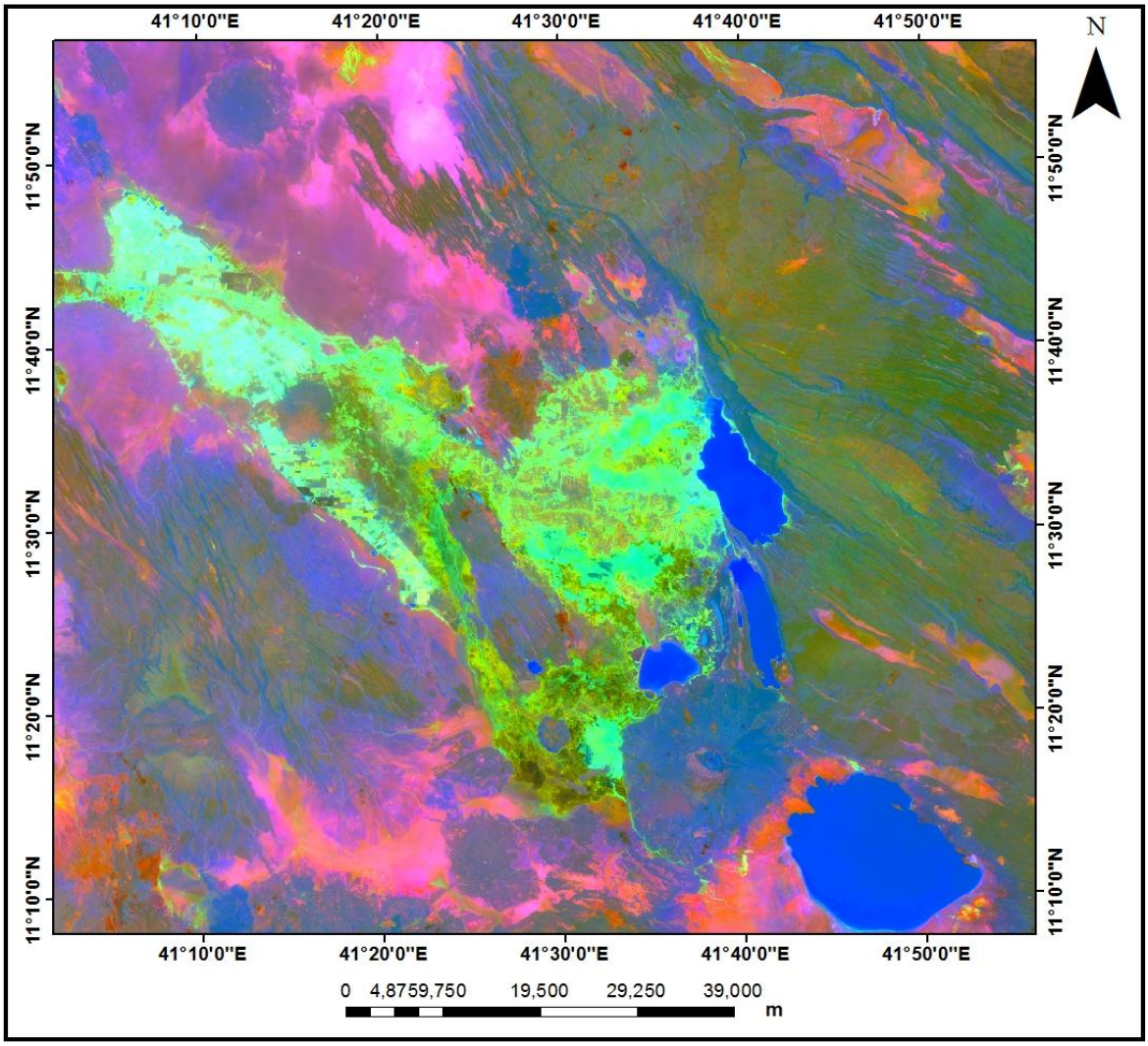

Figure 4.3 Landsat 8 OLI Principal Component Analyses (PC1) Map.

Lithological map were produced by the integration of enhanced false color composite, Intensity hue saturation transformation and Principal component analyses from spectral and spatial characteristics of lithology with the combination of field data results. Six main lithologic units were discriminated this are;

Basaltic unit has found distributed mainly in association with the volcanic centers like Kurub and Demalle volcano near to Lake Abihe in the south east of the study area. The unit contains very fine circular vesicles. This unit is also characterized by many varieties (aphanitic,vesicular, scoracious) and covered large area.

Lava unit has exposed mainly in the southern part of the study area associated with the Damalle and Gabillema volcanic center. Because of lack of accessibility in these localities it was difficult to have an observation point and hence information was acquired only from interpretation of satellite images. It has dark tones on the images, forms hill topography.

The Rhyolite is one of the small area covered lithologic type identified and exposed in different parts of the study by forming ridges and domes. This unit is found in the south at Demalle and Gabillema volcanic areas, and in the north at Serdo village. The rhyolite at all localities have characterized by high degree of deformation exhibiting faults, fractures, and joints. The color of the outcrop varies from dark brown to pink alternatively depending on the degree of weathering.

Evaporates unit was also covered small area and highly exposed along the entire Dobi graben. It covered about 70% of the graben underlying the lacustine sediment exposed on the western escarpment of the Dobi graben. It mostly composed of the exploitable table salt and associated fine grained sediments having white and dull white colors.

Most of the flat lands of the study area specially river channels were covered by Silt, Clay and Sand.. The unit has also exposed along the main road from Mille to Adayitu kebelle. The clay and silt were seen interbedded underlying the sand unit. Based on field observation, the unit has showed varied colors like white, light gray, light brown and gray with off course slight degree of weathering. The texture and grain size varies from clay, silt to sand at all places.

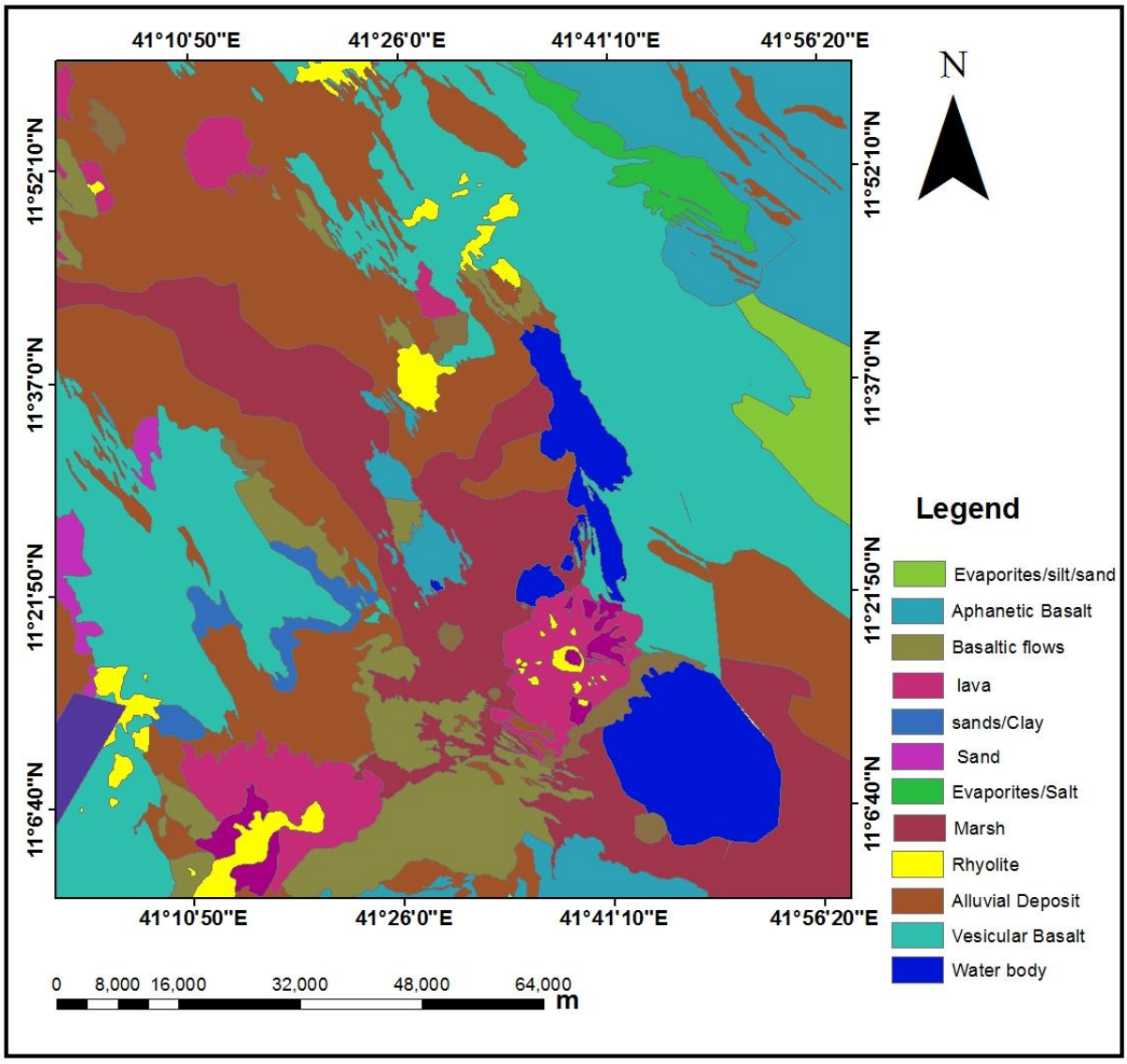

Figure 4.4 Interpreted lithology map of study area.

4.2 Structural Mapping

4.2.1. Convolution Filtering

Across the study area the superposition of different set of brittle structures were identified in all mapped volcanic formations (e. g. regional normal faults to oblique slip faults, shear joints and extensional joints). Spatial enhancements were performed using directional filters for the purpose of lineament and structures analyses. Directional filters were selected for producing effects which may reveal tectonically controlled planar and linear features

4.2.1.1. Gradient-Soble and Gradient-Prewitt Mid-Low Filters of 3 × 3 Window Size Edge Detection

Total 1651minor lineaments are identified in the study area. Table 4.2.and Figure 4.5 showing minor lineaments detected from gradient-soble and gradient-prewitt mid-low filters of 3×3 window size edge detection.

Table 4.2 Filter 3×3 window size edge detection applied.

Soble edge detection 3×3 filter	
horizontally	-1.000 -1.000 -1.000 -1.000 **8.000** -1.000 -1.000 -1.000 -1.000
vertically	-1.000 -1.000 -1.000 2.000 **2.000** 2.000 -1.000 -1.000 -1.000

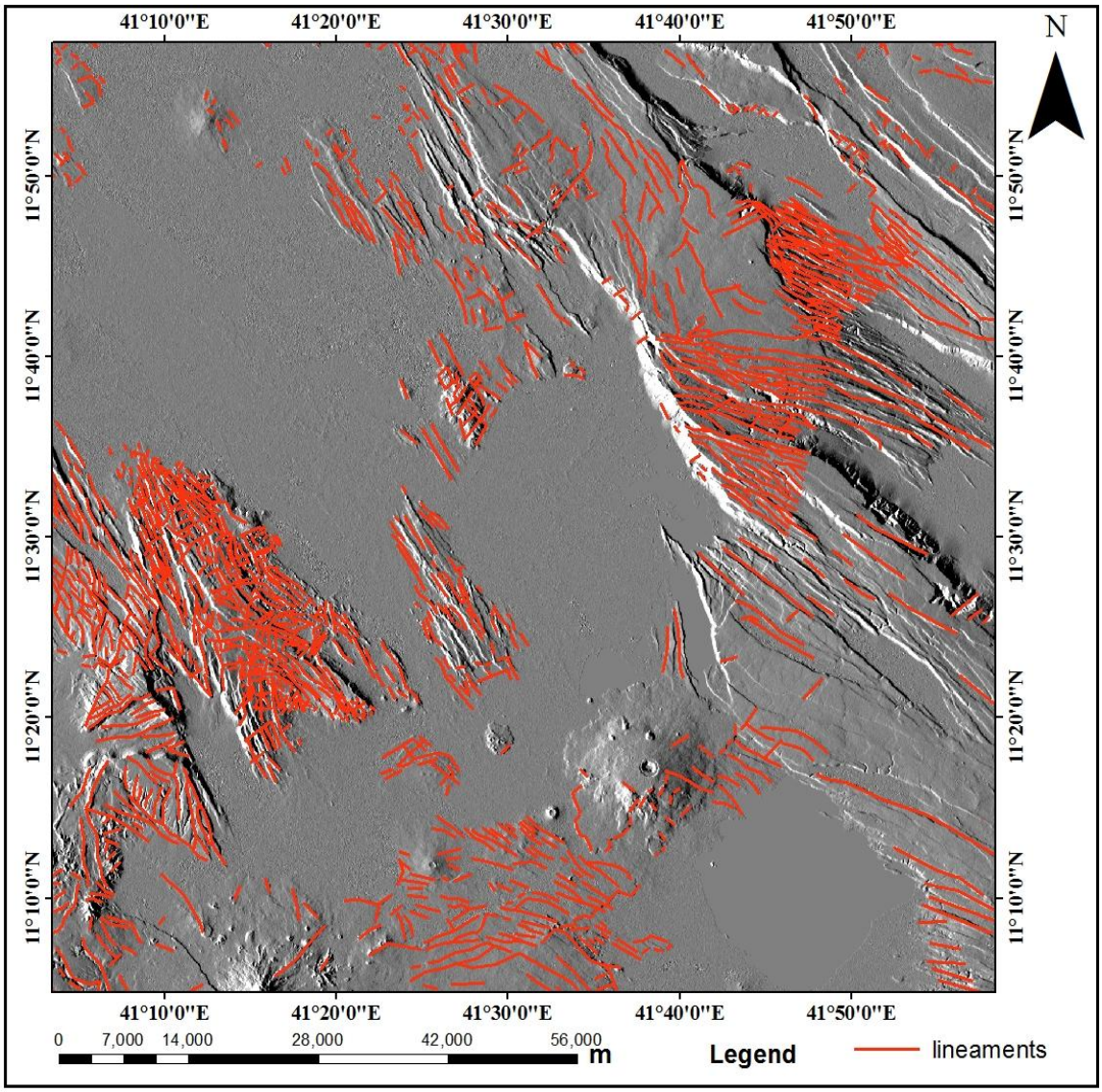

Figure 4.5 Minor lineaments detected from 3×3 window size of edge detection

4.2.1.2 Window Size Directional Filters of 7×7

The major regional faults of the area are the graben bounding faults, which are characterized by high angle with extensive length and throw. Their strikes have actually determined the direction of most of the grabens of the area, with NW as a dominant strike direction. These faults have high throw greater than around 350−400 m east dawn throw and west dawn throw. Totally 56 major faults are identified (Table 4.3 and Fig 4.6) show major faults identified by 7×7 window size directional filters.

Table 4.3 7×7 Window Size Directional Filters applied North–South direction.

7×7 Window Size Directional Filters	
North-South	-1.000-1.000-1.000-1.000-1.000-1.000-1.000 -1.000-2.000-2.000-2.000-2.000-2.000-1.000 -1.000-2.000-3.000-3.000-3.000-2.000-1.000 -1.000-2.000-3.000 **80.000**-3.000-2.000-1.000 -1.000-2.000-3.000-3.000-3.000-2.000-1.000 -1.000-2.000-2.000-2.000-2.000-2.000-1.000 -1.000-1.000-1.000-1.000-1.000-1.000-1.000

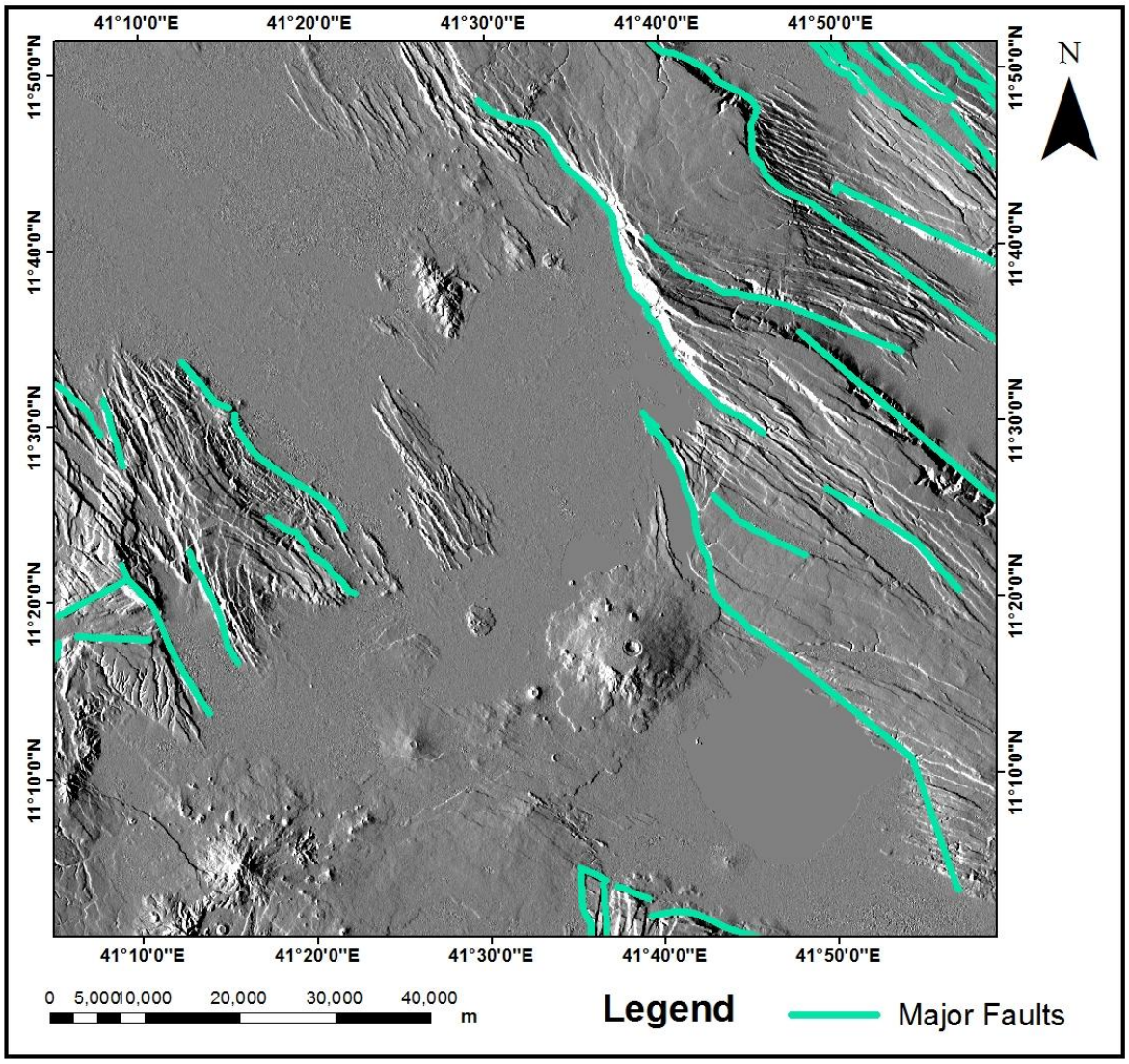

Figure 4.6 Major faults detected from 7×7 window size directional filters.

4.2.1.3. Relief

According to DEM interpolation, local normal faults with different orientation, length and throw (displacement) are the dominant structures in the Study area. From field observation these faults are extensively seen on the vesicular and aphanetic basalts. These faults usually occur together forming a rift-in-rift structure or like step-up faults. The dominant orientations of the faults are ranging from N-NNW direction and geometrically straight-line (less sinuous) and totally 152 normal faults are recognized). Identified kinematics are indicators of slickenside asymmetry reveal a normal movement in the direction of the lineation. Towards the northeast these faults or shear joints dip steeply to the NE and contain steeply to moderately plunging slickenslides. Indicators of normal or oblique left-lateral movement become dominant at around dobi graben .On several localities across the study area these faults appear

to be relatively younger than the major regional faults forming escarpments of the Tendaho and Dobi grabens. Figure 4.7 shows normal faults from relief.

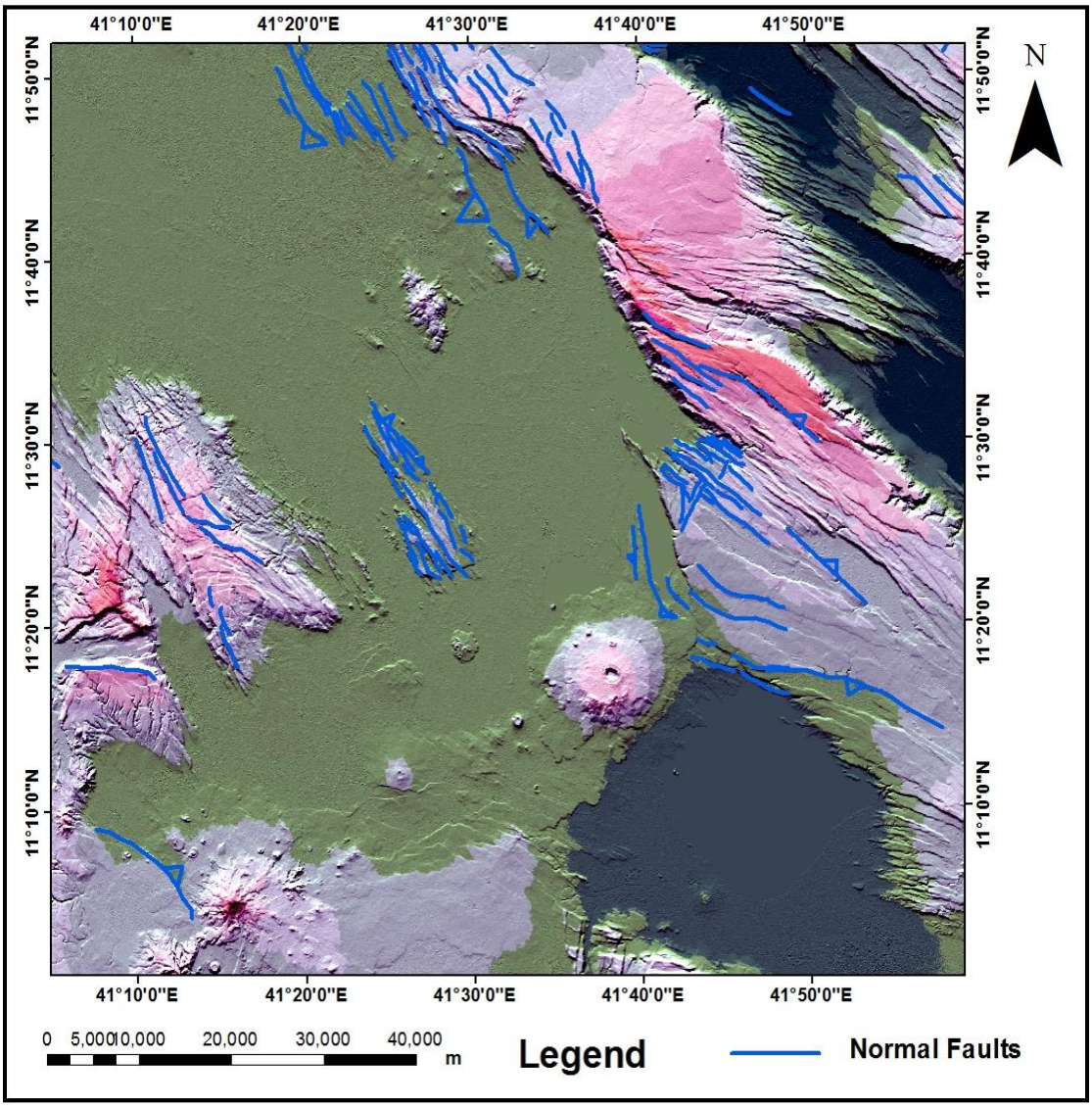

Figure 4.7 Normal Faults from relief map.

4.2.1.3 Aspect and Slope

An aspect and slope map simultaneously showed the aspect (slope direction) and degree (steepness) of terrain slope. High slopes and their associated aspects marked a fault line (strike). Steep slope north (337.5–360) degree of the terrain also marked fault

plane and escarpments. Nine aspects were determined which are aligned in different direction. Figure 4.8 and 4.9 show aspect and slope map of the study area respectively.

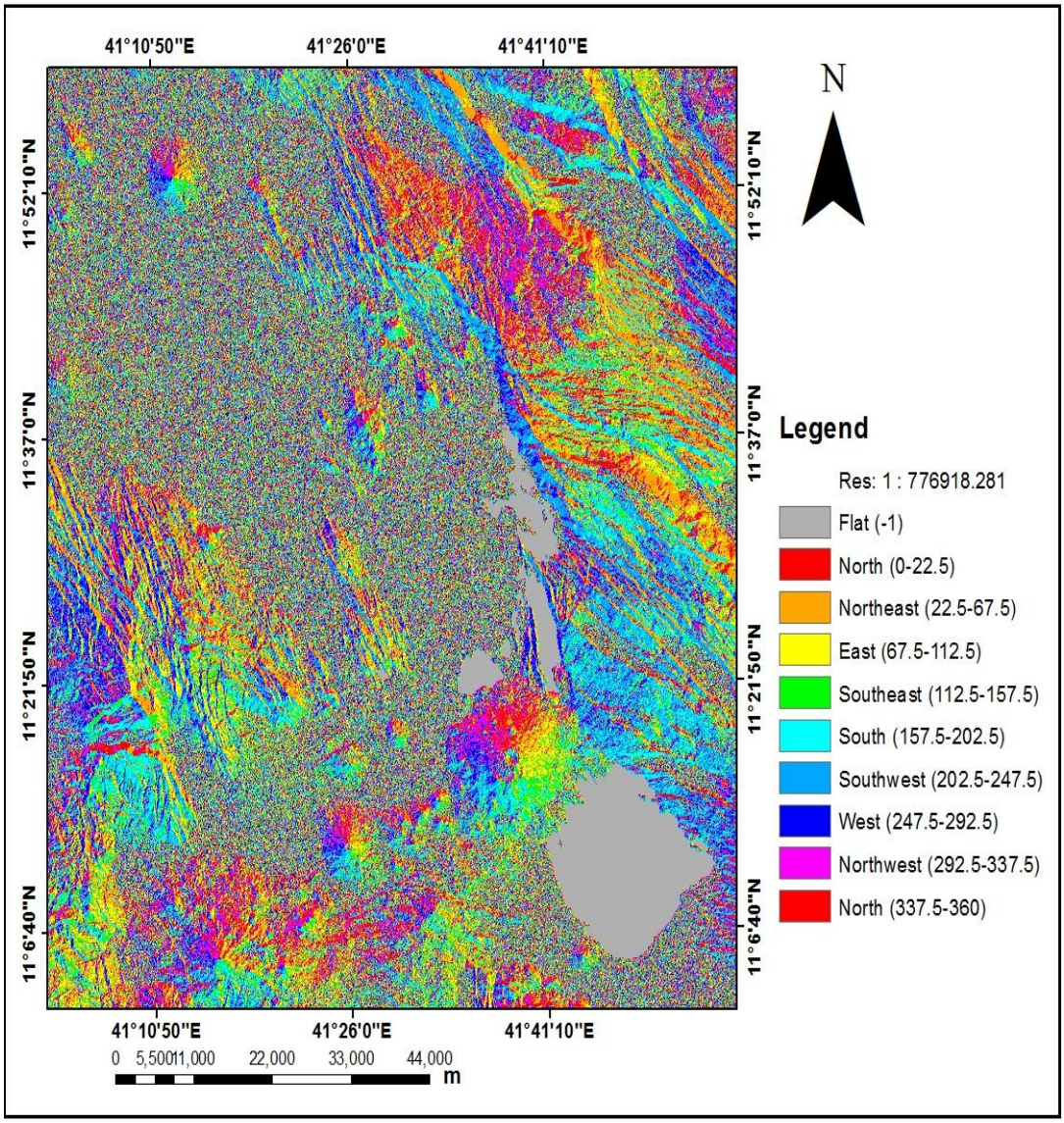

Figure 4.8 Aspect map of study area.

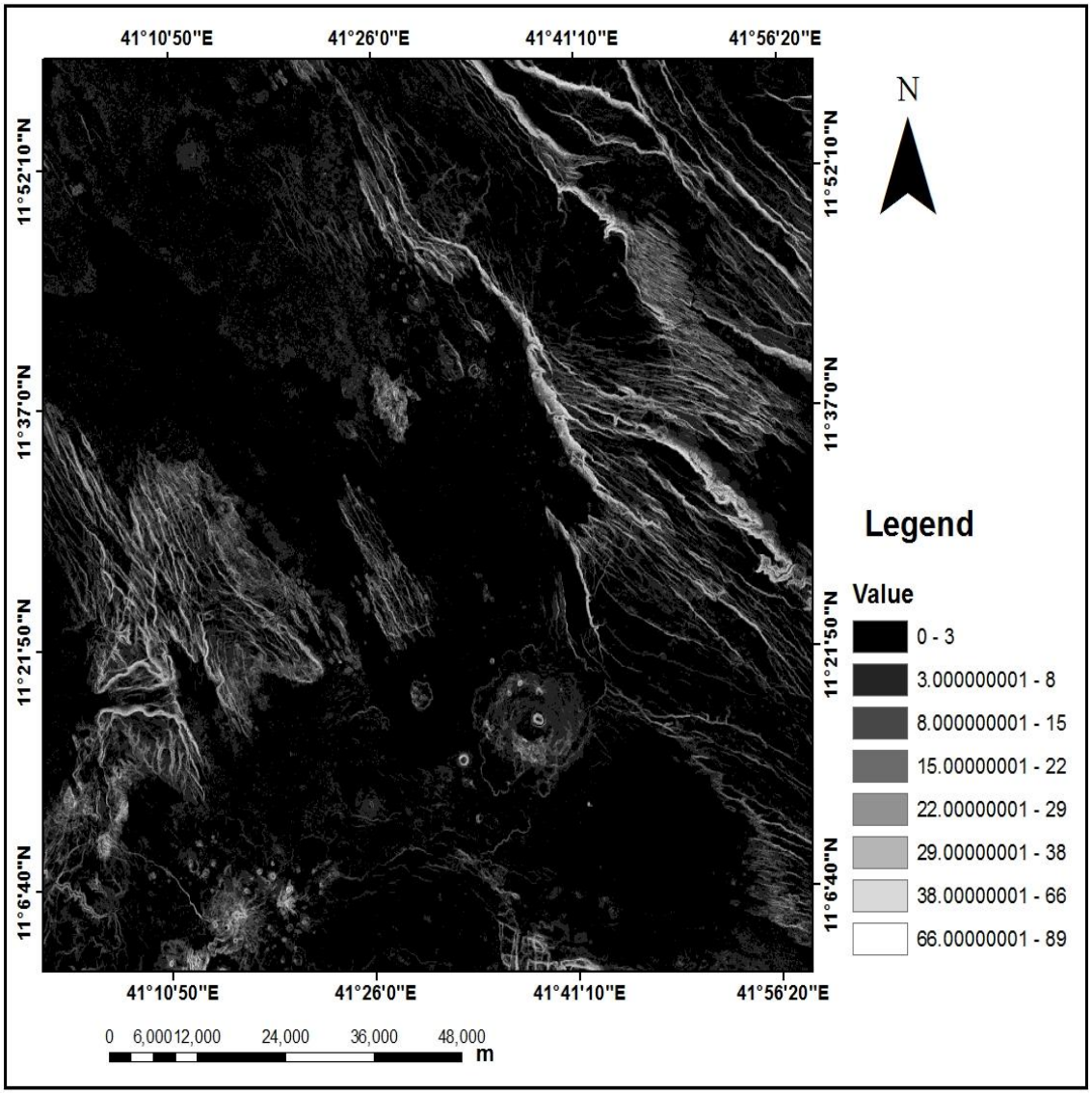

Figure 4.9 slope map of the study area.

Finalized structural map is presented in (Fig.4.10) by the integration of 3×3 window size edge detection,7×7 window size directional filters, aspect map,and painted and relief map.

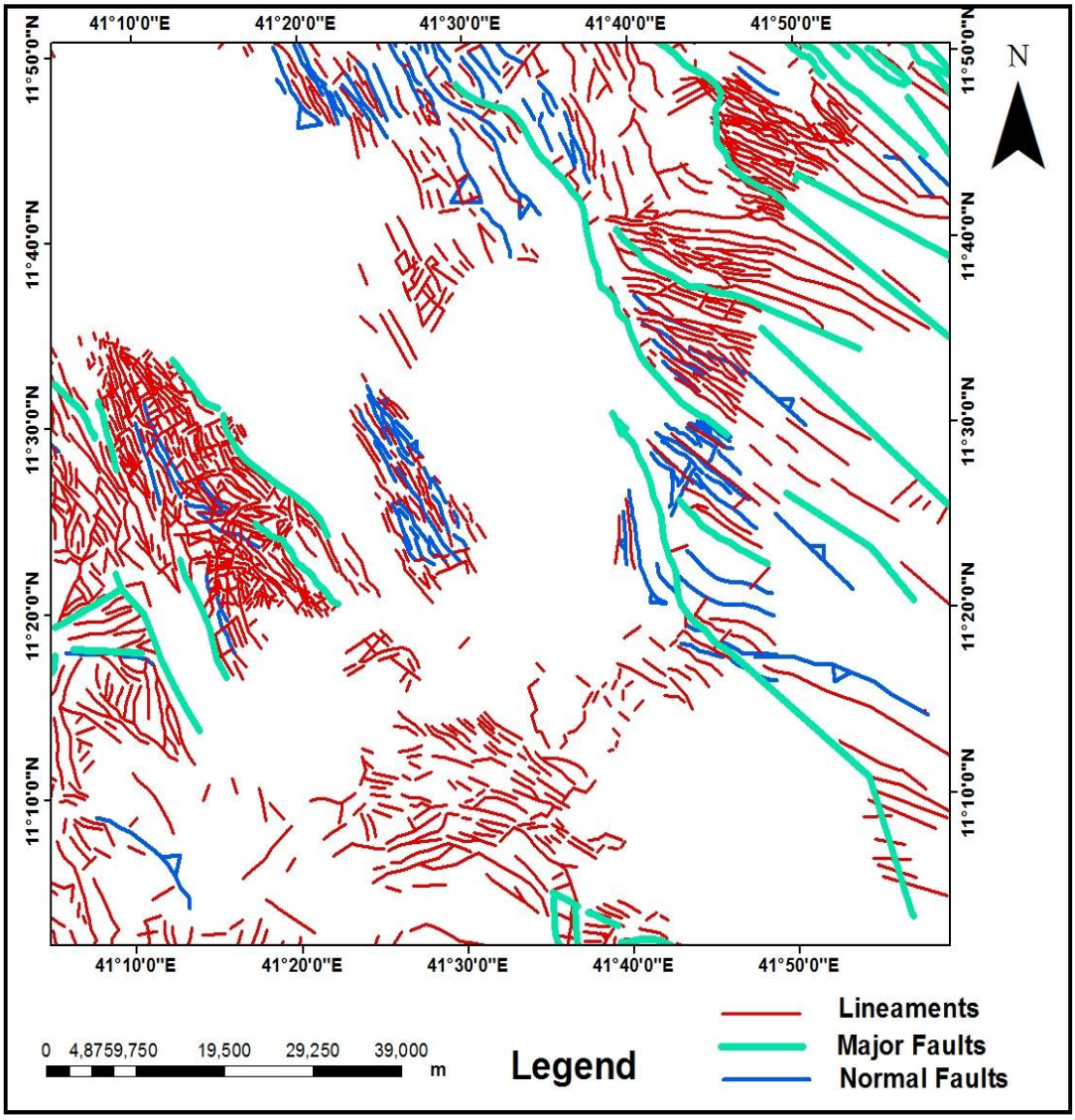

Figure 4.10 Detailed and generalized interpreted structure map of study area.

Tectonism and volcanism create differences in topographic elevations triggering sediment generations that are washed and deposited in rift basins. The lakes and rivers are targets areas for deposition of these sediments, and the plants and animals living in and around them are often buried in the sediments. The building blocks of static geological models are affected by tectonism and volcanism. The litho-stratigraphy of study area is highly controlled by volcanism tectonism and sedimentation processes.

CHAPTER V

DISCUSSION

The use of transformed data space using methods such as PCA and ICA, help to decor relate band information while separating data along new component lines which can further be enhanced by visualizing the new components in FCC

In this study, different digital image processing techniques were applied to landsat 8 Operational Land Imagery, thermal infrared (OLI/TIRS) and Shuttle Radar Topographic Mission Digital Elevation Model (DEM) data aimed to lithological and structural mapping in the study area.

Enhanced false color composite, true color composite image of landsat 8 bands, intensity hue saturation transformation and PCA1 provides best images with overall good lithological information. Enhanced image of input data further enhances the spectral and spatial contrast between different lithologic units and greatly facilitates the visual lithologic interpretation. Thin section mineralogical composition of different rocks units and spectral signature of earth materials obtained from the USGS spectral library, published geological maps and reports also utilized to understand the spectral properties of the different rocks.

Due to the complexity of the geology and little contrast in composition of certain rock or lithologic units, Lithologic interpretation at some places of the processed images was difficult. The typical examples include the lacustrine sediment and alluvial deposit both appear brown color, but well discriminated in the enhanced false color composite image of landsat 8 image and ground truething.

Vegetation covers at the northeast part of the study area masked spectra of rocks in the processed images and make lithologic interpretation difficult. However, slight color variation and morphological difference and field visit helps for lithologic discrimination in this part of the area.

Spatial enhancement of landsat 8 data and topographic information from shuttle radar topographic mission (SRTM) DEM data were found superior methods for structural mapping in this study. Convolution 3×3 and 7×7 window size high frequency edge

detection filters greatly helped to extract surface structures from landsat 8 and DEM data. Shaded-relief (hill-shading) and painted-relief of Shuttle Radar Topographic Mission DEM data provides valuable geomorphologic information for the interpretation of major and minor structures. Grabens and fracture systems are major structural elements recognized from the processed images and DEM data.

The interpreted structural map shows about 1859 structures. The smallest structure size is about 30m and the longest is about 50 km. The interpreted structure map provides the entire small and large structures amount in the study area. The smaller structures indicate joints and lithological contacts. The larger structures indicate the general geometry of faults and other structures and provide information on regional structural patterns.

CHAPTER VI

CONCLUSION AND RECOMMENDATIONS

6 .1 Conclusion

Using landsat 8 data combined with DEM is an effective tool for lithologic and structure detection. Analyzing of Landsat 8 OLI/TIRS and Digital Elevation Model data covering the study area have shown.

- The effectiveness of applying Landsat 8 OLI/TIRS data for geological mapping, through the identification and interpretation of subtle spectral and spatial information difference between different lithologic units.
- The study illustrated the use of landsat 8 and remote sensing data and edge enhancement techniques for lithologic mapping and the applicability of Shuttle Radar Topographic Mission DEM data for mapping geological structures on the basis of their geomorphologic expression.
- The investigation also demonstrates significant implications for geologists to utilize Landsat 8 OLI/TIRS data for geological purposes in the future.

The overall result of this study demonstrates that the Landsat 8 OLI/TIRS and Digital Elevation Model data set can be used as an effective tool for lithological and structural mapping. Although lithological and structural mapping using the satellite remote sensing technique is somewhat hindered by the presence of vegetation cover and the spectral similarities between some of the lithological units caused by the similar vegetation cover, a lithological map with Internal Average Relative Reflectance and structural map with DEM is satisfactory. Therefore, Landsat 8 OLI/TIRS and Digital Elevation Model data can be used to increase lithological and structural discrimination and enhance the overall mapping performance, and to define for any investigation such as, weak zone detection for ground water and engineering geology, targets for mineral exploration, particularly in the area of good rock exposure (very minor soil development and small or absence of vegetation).

6.2 Recommendations

Based on the experience I gained from this study and review of different journal articles, I would like to recommend the following point.

- To explore more detailed surface and subsurface geological information in the study area, it is better to use or apply hyperspectral remote sensing data.
- From observed lithologic properties and abundance of structures, the study area is enriched by the following resources: from alluvial deposit and vesicular basalt ground water, from alluvial sediments fertile soil for agricultural activities, from major consecutive normal faults, geothermal energy sources and hydrothermally altered mineral zones and from evaporates table salt.
- Earth quake is common along this line. Seismic stations are important in this area to regulate earth quake phenomena.

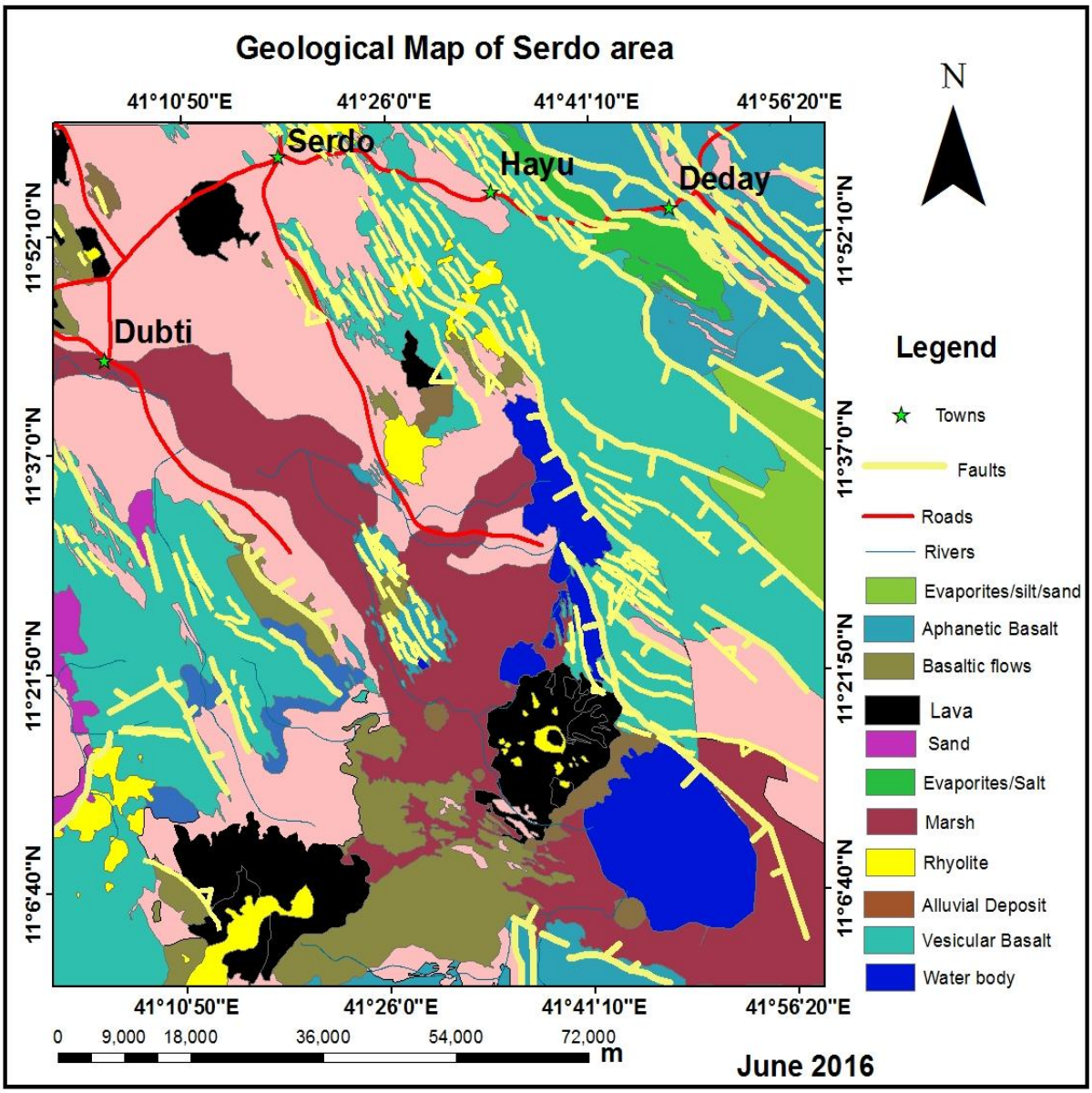

Finalized geological map of Serdo area

Plate1. Rhyolites of the study area

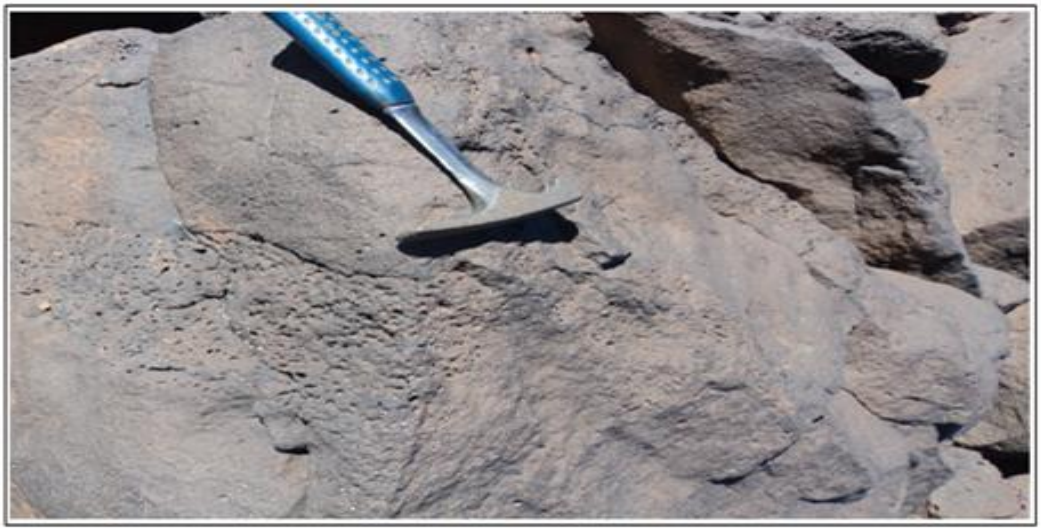

Plate 2 Vesicular Basalt Northern part of the study area.

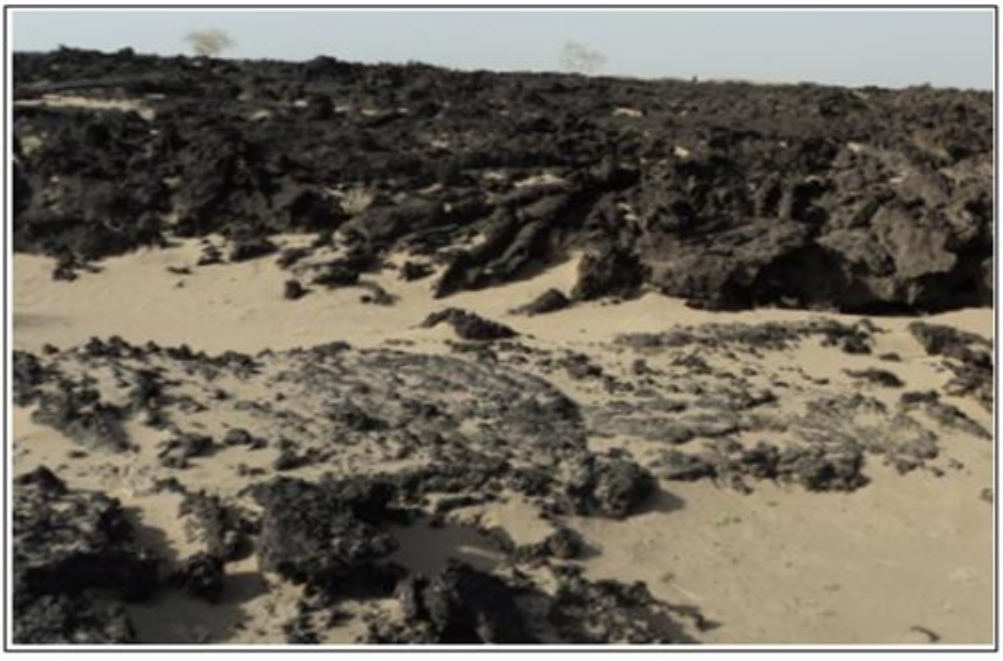

Plate 3 Lava Central part of study area.

Plate 4 Evaporates in the North-Eastern(in Dobi graben) part of the study area.

References

Abdullah, A.,Nassr, S., and Ghaleeb, A. (2013).Remote Sensing and Geographic Information System for Fault Segments Mapping a Study from Taiz Area, Yemen. J. Geol. Res. 2013,1−16.

Argialas, D.,Mavrantza, O., and Stefouli, M. (2003). Automatic mapping of tectonic lineaments (faults) using methods and techniques of Photo interpretation Digita Remote Sensing and Expert Systems.

Abdeen, M.M., Thrurmond, K.A., Abdelsalam, G.M., and Stern, J.R. (2001) Application of ASTER Band-ratio Images for Geological Mapping in Arid Regions: The Neoproterozoic Allaqi Suture, Egypt (Boston,USA).

Abrams, M.J., Rothery, D.A., and Pontual, A., (1988), Mapping in the Oman ophiolite using enhanced Landsat Thematic Mapper images.Tectonophysics, 151, pp. 3874–01.

Acocella,V., Tesfaye. K,and F.Salvini (2003), Formation of normal faults along the axial zone of the Ethiopian Rift, J. Structural. Geol., 25: 503–513.

Alwash, M. A.and Zilger, J., (1994). Remote sensing-based geological mapping of the area west of AlMadinah, Saudi Arabia, International Journal of Remote Sensing, 15: 1, 163–172**.**

Ben-Dor, E.,Kruse, F.A., Lefkoff, A.B. and Banin, A., (1994). Comparison of three calibration techniques for utilization of GER 63-channel aircraft scanner data of Makhtesh Ramon, Nega, Israel. Photogrammetric Engineering and Remote Sensing, 60(11), 1339–1354.

Boardman, J, W., and Kruse F, A.,(1994), Automated spectral Analysis.A geologic example using AVIRIS Data North Grapevine mountains Nevada proceeding of tenth thematic conference on geologic remote sensing.Environmental research of Michigan 1407–1418.

Boccaletti, M., Bonini, M., Mazzuoli, R., Abebe, B., Piccardi, L., and Tortorici, L., (1998), Quaternary oblique extensional tectonics in the Ethiopian Rift (Horn of Africa): Tectonophysics, 287, p. 97–116.

Boccaletti, M., Mazzuoli, R., Bonini, M., Trua, T., and Abebe, B., (1999), Plio–Quaternary volcano tectonic activity in the northern sector of the Main Ethiopian Rift: Relationships with oblique rifting: Journal of African Earth Sciences, v. 29, p. 679– 698.

Boettinger, J.L., Ramsey, R.D., Bodily, J.M., Cole, N.J., Kienast-Brown, S., Nield, S.J., Saunders, A.M., and Stum, A.K.(2008).Landsat Spectral Data for Digital Soil Mapping. In Digital Soil Mapping with Limited Data, A.E. Hartemink, A. McBratney, and M. de L. Mendonça-Santos, eds. (Dordrecht: Springer Netherlands), pp. 193–202.

Campbell, J.B.(2002).Band ratios. In Introduction to Remote Sensing, (New York: Guilford Press), p. 505.

Campbell, J.B.(2009).Remote sensing of Soils. In The Sage Handbook of Remote Sensing,(Thousand Oaks, CA: Sage), pp. 341–354.

Carranza, E.J.M., and Hale, M.(2002).Mineral imaging with Landsat Thematic Mapper data for hydrothermal alteration mapping in heavily vegetated terrain. Int. J.Remote Sens. *23*, 4827– 4852.

Corti. G, *et al*.(2013) Re-orientation of the extension direction and pure extensional faulting at oblique rift margins: comparison between the Main Ethiopian Rift and laboratory experiments. Terra Nova, 25,. 5, 396–404.

Chavez, P. S., Berlin, G.L.,and Sowers, L.B. (1982).Statistical method for selecting Landsat MSS ratios.Journal of Applied Photograph Eng., 8, 23–30.

Chaabouni, R., Bouaziz, S., Peresson, H.,and Wolfgang, J. (2012).Lineament analysis of South Jenein Area (Southern Tunisia) using remote sensing data and geographic information system. Egypt. J. Remote Sens. Space Sci. 15, 197–206.

Crane, R. B. (1971).Processing techniques to reduce atmospheric and sensor variability in multispectral scanner data. Proceeding 7th International symposium Remote Sensing and Environment, 2,1345–1355.

Cortez, L., Durão, F., and Ramos, V.(1997).Testing some Connectionist Approaches for Thematic Mapping of Rural Areas. In Neurocomputation in Remote Sensing Data Analysis, I. Kanellopoulos, G.G. Wilkinson, F. Roli, and J. Austin, eds. (Berlin, Heidelberg: Springer Berlin Heidelberg), pp. 142–150.

Chen, X., and Campagna, D.J. (2009).Remote Sensing of Geology. In The Sage Handbook of Remote Sensing, (Thousand Oaks, CA: Sage), pp. 328–340.

Drury, S ,A., (1987). Image Interpretation in Geology, 66-148 (Kluwer Academic Publishers) 296 pp.

Drury, S.A. (1993). Image interpretation in geology (London; New York: Chapman & Hall).

Ebinger, C.J., 1989: Tectonic development of the western branch of the East African rift system.Geol. Soc. Am. Bull.101: 885–903.

Ebinger, C.J., Yemane, T., Wolde Gabriel, G., Aronson, J.L., and Walter, R.C., (1993), Late Eocene Recent volcanism and faulting in the southern main Ethiopian rift: Geological Society (London) Journal, v. 150, p.99–108.

Ebinger, C. J., and Hayward, N., J. (1996), Soft plates and hot spots: Views from Afar,J. Geophys. Res., 101:21,859–21,876.

Ebinger, C. J., and M. Casey (2001), Continental break up in magmatic provinces: An Ethiopian example, Geology, 29: 5275–30.

Ebinger, C., *et al*.,(2010). Length and Timescales of Rift Faulting and Magma Intrusion: The Afar Rifting Cycle from 2005 to Present. Annu. Rev. Earth Planet, Sci. 38: 439–66.

Ethiopian Mapping Agency (2016) (Addis Ababa Ethiopia)

Favretto, A., Geletti, R., and Civile, D. (2013). Remote sensing as a preliminary analysis for the detection of active tectonic structures: an application to the Albanian orogenic system. Geoadria *18*, 97–111.

Ferguson, D.J., *et al*., Recent rift related volcanism in Afar, Ethiopia, Earth Planet. Sci. Lett. (2010).

Gillespie, A. R., Kahle, A. B. and Walker, R. E.(1986). Color enhancement of highly correlated images, decorrelation and IHS contrast stretches. Remote Sensing Environment, 2, 209–235.

Gad, S., and Kusky, T. (2006). Lithological mapping in the Eastern Desert of Egypt, the Barramiya area, using Landsat thematic mapper (TM). J. Afr. Earth Sci.44, 196–202.

Geological Survey of Ethiopia (Addis Ababa Ethiopia)

Gudmundsson, A. (1995), Infrastructure and mechanics of volcanic systems in Iceland.

Gudmundsson, A. (1998), Magma chambers modeled as cavities explain the formation of rift zone central volcanoes and their eruption and intrusion statistics.

Harris, J.R., Eddy, B., Rencz, A.,de Kemp, E., Budketwitsch, P., and Peshko, M. (2001).Remote sensing as a geological mapping tool in the Arctic: preliminary results from Baffin Island, Nunavut. Current Research 200–1E12, 13

Hook, J. H., Dmochowski, J.E., Howard, K.A., Rowan, L.C., Karlstrom, K.E., Stock J.M., (2005). Mapping variations in weight percent silica measured thermal infrared imagery-Examples from Hiller Mountains, Nevada, USA and Tres Virrgenes-La Reforma, Baja California Sur, Mexico. Remote Sensing of Environment, 99(1–2):237–298.

Inzana, J., Kusky, T., Higgs, G., Tucker, R., 2003. Supervised classifications of Landsat TM band ratio images and Landsat TM band ratio image with radar for geological interpretations of central Madagascar. Journal of African Earth Sciences.37, 59–72.

Jones, A,R.,(1996), An Evaluation of satellite thematic mapper imagery for geomorphological mapping in arid and semi arid environment.International geomorphology.Edited by Gardiner V (Chichester. Wiley) p 343–357.

Jensen, J. R., (1996). Introductory Digital Image Processing. Prentice Hall Seriesin Geographic Information Science,New Jersey, 316p.

Kenea, N.H.,(1997). Improved geological mapping using LandsatTM data, Southern Red Sea Hills,Sudan: PC and HIS decorrelation stretching. Int. J. Remote Sens.18, 12331– 244.

Kazmin, V. G., and A. F. Bacon (2000), Magmatism and crustal accretion in continental rifts, J. Afr. Earth Sci., 30 : 555 5–68.

Kruse, A.F. (1998). Advances in Hyperspectral Remote Sensing for Geologic Mapping and Exploration In 9th Australasian Remote Sensing Conference, (Sydney, Australia).

Kruse, A. F., Boardman, J, W., and Huntington, J, F., (2003), Comparison of Airborne Hyper spectral data and EO-1 Hyperion for mineral mapping. IEE Transaction in Geosciences and remote sensing (special issue). 41(6); 1388–1400.

Landsat 8 Data Users Handbook June (2015) Department of the interior U.S. Geological Survey

Laake, A. (2011). Integration of satellite imagery, Geology and geophysical Data. In Earth and Environmental Sciences, (INTECH Open Access Publisher), pp. 467–492

Lahitte, P., P. Y. Gillot, and V. Courtillot, (2003a), silicic central volcanoes as precursors to rift propagation: The Afar case, Earth Planet. Sci. Lett., 207:10311–6.

Le Gall, B., J. (2000), A morphotectonic study of an extensional fault zone in a magma rich rift: The Baringo Trachyte Fault System, central Kenya Rift, Tectonophysics, 320, 8710–6.

Lillesand, T.M. Kiefer, R.W. and Chipman, J.W.(2004) Remote Sensing and Image Interpretation, 5th Ed., John Wiley and sons Inc. New York,ISBN 0–471–25515–7, 763P.

List, F. K.(1993).Fundamentals of digital image processing for geological application, Proceeding of the 4th United Nations Ins.Training Course on Remote Sensing Application to Geological Science. Berliner Geowiss Abh. D,5, 7–29.

Liu, C. C., Sousa Jr., M. A. and Gopinath,T.R. (2000). Regional structural analysis by remote sensing for mineral exploration, Paraiba state, Northern Brazil.Geocarto International,15, 69–75.

Macdonald, K.C., (1998). Linkages between faulting,volcanism, hydrothermal activity and segmentation on fast spreading centres. In: Faulting and Magmatism at Mid-Ocean Ridges. American Geophysical Union,Washington, DC, pp. 275–8.

Macias, L, F. (1995), Remote sensing of Mafic Ultramafic rocks Example from Australian Precambrian terrain . Journal of Australian Geology and Geophysics 16:163–171.

Marco, R, (2007).Remote sensing capability in structural geology analysis of different geodynamic settings: Scientifica Acta 1, No. 1, 43–46.

Maina-Gichaba,C., Kipseba, E.K., and Masibo, M.(2013).Overview of Landslide Occurrences in Kenya. In Developments in Earth Surface Processes,(Elsevier), pp. 293–314.

Marghany, M.,and Hashim, M. (2010).Lineament mapping using multispectral remote sensing satellite data. Int. J.Phys.Sci.5,15011–507.

Mia, B., and Fujimitsu, Y. (2012).Mapping hydrothermal altered mineral deposits using Landsat 7 ETM+ image in and around Kuju volcano, Kyushu, Japan. J. Earth Syst. Sci. 121, 1049–1057.

Mwaniki, M.W., Moeller, M.S.,and Schellmann, G. (2015).Application of remote sensing technologies to map the structural geology of central Region of Kenya. IEEE J. Sel. Top. Appl. Earth Obs. Remote Sens. soon.

Meyer, W., Pilger, A., Rosler, A., and Stets, J., (1975), Tectonic evolution of the northern part of the Main Ethiopian Rift in southern Ethiopia, *in* Pilger, A.,and Rosler,A.,eds., Afar Depression of Ethiopia: Stuttgart, Germany , Schweizerbart, Scientific Report 14, p. 352–362.

Mohr, P. A. (1972).Surface structure and plate tectonics of Afar,Tectonophysics, 15,318.

Mohr, P.A. and Wood, C.A.,(1976).Volcano spacing and lithospheric attenuation in the eastern rift of Kenya. Earth and Planetary Science Letters, 3:126–144.

Mohr, P., Zanettin, B., (1988).The Ethiopian flood basalt province. In: Macdougall , J.D.(Ed), Continental flood basalts Kluwer Academic Publishers, pp. 63–110.

Nama, E. E, (2004). Lineament detection on Mount Cameroon during the 1999 volcanic eruptions using Landsat ETM *I*nternational Journal of Remote Sensing, 25: 501–510.

Ninomiya,Y., Fu, B., and Cudahy, T.J.(2005).Detecting lithology with Advanced Spaceborne Thermal Emission and Reflection Radiometer (ASTER) multispectral thermal infrared “radiance at sensor” data. Remote Sens. Environ. 99,127–139.

Pour, B. A., Hashim, M, and van Genderen. J.(2013). Detection of hydrothermal alteration zones in a tropical region using satellite remote sensing data: Bau gold field, Sarawak, Malaysia. Ore Geology Reviews. 54, 181–196.

Pour, B. A., Hashim, M, Marghany. M.,(2014). Exploration of gold mineralization in a tropical region using Earth Observing-1 (EO1) and JERS-1 SAR data: a case study from Bau gold field, Sarawak, Malaysia.Arabian Journal of Geosciences. 7, 2393–2406.

Ramli, M.F., Yusof, N., Yusoff, M.K., Juahir, H., and Shafri, H.Z.M. (2010). Lineament mapping and its application in landslide hazard assessment: a review. Bull. Eng. Geol. Environ. *69*, 215–233.

Rajesh, H.M. (2004). Application of remote sensing and GIS in mineral resource mapping An overview. Journal of Mineralogy and Petrological Sciences, 99, 83–203,.

Rahnama, M., and Gloaguen, R. (2014). Tec Lines: A MATLAB-Based Toolbox for Tectonic Lineament Analysis from Satellite Images and DEMs, Part 1: Line Segment Detection and Extraction. Remote Sens. 6: 5938–5958.

Rajendran, S., Thirunavukkaraasu, A., Poovalingaganesh, B.,Kumar, K.V., and Bhaskaran, G.(2007).Discriminationof lowgrade magnetite ores using remote sensing techniques. J. Indian Soc. Remote Sens. 35: 153–162.

Rein, B. and Kufmann, H. (2003). Exploration for gold using panchromatic stereoscopic intelligence satellite photographs and Landsat TM daa in the Hebi area,china. International Journal of Remote Sensing, 24:2427–2438.

Rencz,A,L., Bowie,C., and Ward,B.,(1996),Aplication of thermal imagery for identification of kimberlites . Lac De Grass area District of Mackenzi NWT in Lechainment AN Richard son DG,Dilabio RNW, Richardson KA(eds) searching for Diamond in Canada geological survey Canada 255–258

Rothery, D.A., (1987).The role of Landsat multispectral scanner (MSS) imagery in mapping the Oman ophiolite. Journal of Geological Society of London, 144, pp.587–597.

Roy, D.P., Wulder, M.A., Loveland, T.R., C.E., W., Allen, R.G., Anderson, M.C., Helder, D., Irons, J.R., Johnson, D.M., Kennedy, R., et al. (2014). Landsat8 Science and product vision for terrestrial global change research. Remote Sens. Environ. 145, 154–172.

Sabins, F. F., (1987). Remote Sensing Principles and Interpretation, 2nd ed., 449 pp.

Sabins, F.F. , (1997). Remote sensing: principles and interpretation (New York: W.H. Freeman and Company).

Sabins, F.F., (1999).Remote sensing for mineral exploration. Ore Geol. Rev. 14,157–183.

Skidmore, A., (1989).A comparison of techniques for calculating gradient and aspect from a gridded digital elevation model. International Journal of Geographical Information Systems, 3(4):3233–34.

Sultan,M., Arvidson, R.E., Sturchio, N.C., and Guinness, E.A. (1987). Lithologic mapping in arid regions with Landsat thematic mapper data: Meatiq dome, Egypt. Geol. Soc. Am . 99,748.

Suzen,M.L., and Toprak, V. (1998). Filtering of satellite images in geological lineament analyses: An application to a fault zone in Central Turkey. Int.J.Remote Sens.19,1101–1114.

Short, N.M.Sr., and Blair, R.W.Jr. (eds.) (1986), Geomorphology from Space, NASA

Tazieff, H., Varet, J. (1972).Tectonic significance of the Afar (or Danakil) Depression. Nature 235, 144–147.

Vinod, K, K., (2006), Detection of volcanic eruption in Barren Iceland using IRS AWIFS data. Current science 91(6):752–753.

Williams, F. M., M. A. J. Williams, and F. Aumento (2004), Tensional fissures and crustal extension rates in the northern part of the Main Ethiopian Rift, J. Afr. Earth Sci., 38:183–197.

Wolde Gabriel, G., Aronson, J., Walter, R.C.(1990), Geology, geochronology, and rift basin development in the central sector of the Main Ethiopian Rift, Geol. Soc. Am. Bull. 102: 439–458.

Wolfenden, E., Ebinger, C., Gezahegn, Y., Deino, A., and Dereje, A.,(2004), Evolution of the northern Main Ethiopian Rift: Birth of a triple junction, Earth Planet. Sci.Lett.,224: 213 2–28.

United State Geological Survey (2015) USA,(https://earthexplorer.usgs.gov).

D E C L A R A T I O N

I hereby declare that the thesis entitled “Identification of lithology and structures in Serdo, Afar, Ethiopia and their Static Geological Model using Remote Sensing And GIS Techniques” has been carried out by me under the supervision of Dr. K.V. Suryabhagavan, Associate Professor, School of Earth Sciences, College of Natural and Computational Sciences, Addis Ababa University, Addis Ababa during the year 2015−2016 as a part of Master of Science program in Remote Sensing and GIS. I further declare that this work has not been submitted to any other University or Institution for the award of any degree or diploma.

Addis Seid Jibril

Signature: _____

Addis Ababa University

Addis Ababa

Ethiopia

Date: June, 2016

C E R T I F I C A T E

This is certified that the thesis entitled “Identification of lithology and structures in Serdo, Afar, Ethiopia and their Static Geological Model using Remote Sensing and GIS Techniques” is a bonafied work carried out by Addis Seid Jibril under my guidance and supervision. This is the actual work done by Addis Seid for the partial fulfillment of the award of the Degree of Master of Science in Remote Sensing and GIS from Addis Ababa University. Addis Ababa, Ethiopia.

Dr. K. V. Suryabhagavan

Associate Professor

Signature: _____

School of Earth Sciences

Addis Ababa University

Addis Ababa

Date: May, 2016